

MAR 04 1986

AEDC-TR-85-50

C.3



Empirical Development of Ground Acceleration, Velocity, and Displacement for Accidental Explosions at J5 or the Proposed Large Altitude Rocket Cell at Arnold Engineering Development Center

Barbara C. Davis
Lawrence Livermore National Laboratory
University of California
Livermore, CA 94550

PROPERTY OF U.S. AIR FORCE
AEDC TECHNICAL LIBRARY

**TECHNICAL REPORTS
FILE COPY**

December 1985

Final Report for Period October 1983 – September 1984

Approved for public release; distribution unlimited.

**ARNOLD ENGINEERING DEVELOPMENT CENTER
ARNOLD AIR FORCE STATION, TENNESSEE
AIR FORCE SYSTEMS COMMAND
UNITED STATES AIR FORCE**

NOTICES

When U. S. Government drawings, specifications, or other data are used for any purpose other than a definitely related Government procurement operation, the Government thereby incurs no responsibility nor any obligation whatsoever, and the fact that the government may have formulated, furnished, or in any way supplied the said drawings, specifications, or other data, is not to be regarded by implication or otherwise, or in any manner licensing the holder or any other person or corporation, or conveying any rights or permission to manufacture, use, or sell any patented invention that may in any way be related thereto.

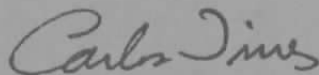
Qualified users may obtain copies of this report from the Defense Technical Information Center.

References to named commercial products in this report are not to be considered in any sense as an endorsement of the product by the United States Air Force or the Government.

This report has been reviewed by the Office of Public Affairs (PA) and is releasable to the National Technical Information Service (NTIS). At NTIS, it will be available to the general public, including foreign nations.

APPROVAL STATEMENT

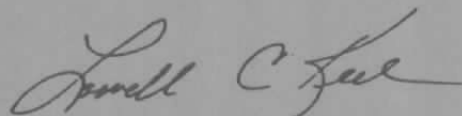
This report has been reviewed and approved.



CARLOS TIRRES
Facility Technology Division
Directorate of Technology
Deputy for Operations

Approved for publication:

FOR THE COMMANDER



LOWELL C. KEEL, Lt Colonel, USAF
Director of Technology
Deputy for Operations

UNCLASSIFIED

SECURITY CLASSIFICATION OF THIS PAGE

REPORT DOCUMENTATION PAGE

1a REPORT SECURITY CLASSIFICATION UNCLASSIFIED		1b RESTRICTIVE MARKINGS	
2a SECURITY CLASSIFICATION AUTHORITY		3 DISTRIBUTION/AVAILABILITY OF REPORT Approved for public release; distribution is unlimited.	
2b DECLASSIFICATION/DOWNGRADING SCHEDULE			
4. PERFORMING ORGANIZATION REPORT NUMBER(S) AEDC-TR-85-50		5. MONITORING ORGANIZATION REPORT NUMBER(S)	
6a. NAME OF PERFORMING ORGANIZATION Lawrence Livermore National Laboratory	6b. OFFICE SYMBOL <i>(if applicable)</i>	7a. NAME OF MONITORING ORGANIZATION	
6c. ADDRESS (City, State and ZIP Code) University of California Livermore, CA 94550		7b. ADDRESS (City, State and ZIP Code)	
8a. NAME OF FUNDING/SPONSORING ORGANIZATION Arnold Engineering Development Center	8b. OFFICE SYMBOL <i>(if applicable)</i> DOT	9. PROCUREMENT INSTRUMENT IDENTIFICATION NUMBER FY7483-83-0007	
8c. ADDRESS (City, State and ZIP Code) Air Force Systems Command Arnold Air Force Station, TN 37389-5000		10 SOURCE OF FUNDING NOS	
11. TITLE (Include Security Classification) Please see reverse of this page.		PROGRAM ELEMENT NO. 65807F	TASK NO.
		PROJECT NO.	WORK UNIT NO.
12. PERSONAL AUTHOR(S) Davis, Barbara C., Lawrence Livermore National Laboratory			
13a. TYPE OF REPORT Final	13b. TIME COVERED FROM 10/83 TO 9/84	14. DATE OF REPORT (Yr, Mo, Day) December 1985	15. PAGE COUNT 40
16. SUPPLEMENTARY NOTATION Available in Defense Technical Information Center (DTIC).			
17. COSATI CODES		18. SUBJECT TERMS (Continue on reverse if necessary and identify by block number)	
FIELD	GROUP	SUB GR	
08	11	ground shock displacement	
19	04	ground motion blast damage	
		acceleration	
19. ABSTRACT (Continue on reverse if necessary and identify by block number)			
<p>This study is an assessment of the ground shock which may be generated in the event of an accidental explosion at J5 or the proposed Large Altitude Rocket Cell (LARC) at the Arnold Engineering Development Center (AEDC). The assessment is accomplished by reviewing existing empirical relationships for predicting ground motion from ground shock. These relationships are compared with data for surface explosions at sites with similar geology and with yields similar to expected conditions at AEDC. Empirical relationships are developed from these data and a judgment made whether to use existing empirical relationships or the relationships developed in this study.</p> <p>An existing relationship (Lipner et al.) is used to predict velocity; the empirical relationships developed in the course of this study are used to predict acceleration and displacement. The ground motions are presented in table form and as contour plots. Included also is a discussion of damage criteria from blast and earthquake studies.</p> <p>This report recommends using velocity rather than acceleration as an indicator of</p>			
20. DISTRIBUTION/AVAILABILITY OF ABSTRACT UNCLASSIFIED/UNLIMITED <input type="checkbox"/> SAME AS RPT <input checked="" type="checkbox"/> DTIC USERS <input type="checkbox"/>		21. ABSTRACT SECURITY CLASSIFICATION UNCLASSIFIED	
22a. NAME OF RESPONSIBLE INDIVIDUAL W.O. Cole		22b. TELEPHONE NUMBER <i>(Include Area Code)</i> (615) 454-7813	22c. OFFICE SYMBOL DOS

UNCLASSIFIED

SECURITY CLASSIFICATION OF THIS PAGE

11. TITLE. Concluded.

Empirical Development of Ground Acceleration, Velocity, and Displacement for Accidental Explosions at J5 or the Proposed Large Altitude Rocket Cell at Arnold Engineering Development Center

19. ABSTRACT. Concluded.

structural blast damage. It is recommended that $v = 2$ ips ($v = .167$ fps) be used as the damage threshold value (no major damage for $v < 2$ ips).

UNCLASSIFIED

SECURITY CLASSIFICATION OF THIS PAGE

Preface

The work reported herein was conducted by Lawrence Livermore National Laboratory (LLNL), Livermore, CA 94550, under MIPR number FY7483-83-0007 for the Director of Technology (DOT), Arnold Engineering Development Center (AEDC), Air Force Systems Command (AFSC), Arnold Air Force Station, Tennessee, during the period October 1983 to September 1984. The Project Manager was Mr. Carlos Tirres, AEDC/DOT. Ray Pierce was the Project Manager for LLNL. Bob Murray was the Project Leader for this task, and Don Bernreuter provided consultation and technical direction.

Contents

Preface	ii
List of Illustrations	iv
List of Tables	v
Abstract	1
Introduction	1
Site Description	1
Surface Burst Ground Shock Phenomenology	3
Study Methodology	6
Comparison of Predicted Values to Specific Sites	11
Acceleration Comparisons	11
Velocity Comparisons	12
100T TNT Equivalent Yield Events	12
20T TNT Equivalent Yield Events	12
Displacement Comparisons	13
Results	19
Discussion of Damage Indicators	29
Maximum Acceleration as an Indicator of Damage	29
Maximum Velocity as an Indicator of Damage	29
Recommendations	29
References	35
Bibliography	35

List of Illustrations

1. The AEDC Complex.....	2
2. Site for the proposed LARC facility at AEDC.....	4
3. 15T [1] and 50T [2] equivalent (2.0 weighting factor) surface burst close-in peak DI/CI acceleration for generic wet site	7
4. 50T TNT equivalent (2.0 weighting factor) surface burst peak DI/CI velocity [1] and peak ground roll velocity [2] for generic wet site	8
5. 15T TNT equivalent (2.0 weighting factor) surface burst peak DI/CI velocity [1] and peak ground roll velocity [2] for generic wet site	9
6. 50T TNT equivalent surface burst peak DI/CI displacement [1] and peak ground roll displacement [2] for generic wet site	10
7. 15T TNT equivalent surface burst peak DI/CI displacement [1] and peak ground roll displacement [2] for generic wet site	11
8. Near-surface peak vertical acceleration for surface and surface-tangent 20T high explosive events at wet, layered sites: Generic w/2.0 yield weighting [1], Least-squares regression [2], Sauer and Schoutens PPG [3], Sauer and Schoutens NTS [4] peak vertical acceleration relationships	13
9. Near-surface peak horizontal acceleration for surface and surface-tangent 20T high explosive events at wet, layered sites: Generic w/2.0 yield weighting [1], Least-squares regression [2], Sauer and Schoutens PPG [3], Sauer and Schoutens NTS [4] peak horizontal acceleration relationships	14
10. Near-surface peak velocity for surface tangent 100T high explosive events at wet, layered sites: Sauer HE [1], Generic Ground Roll [2a], Generic Ground Roll w/2.0 yield weighting [2b], Sauer PPG [3], Sauer NTS [4] peak velocity relationships	15
11. Near-surface peak velocity for surface and surface-tangent 20T high explosive events at wet, layered sites: Sauer PPG [1], Sauer NTS [2], Generic Ground Roll [3a], Generic Ground Roll w/2.0 yield weighting [3b] peak velocity relationships	16
12. Near-surface peak vertical displacement for high explosive events at wet, layered sites: Least-squares regression [1], Sauer and Schoutens PPG [2]	17
13. Near-surface peak horizontal displacement for high explosive events at wet, layered sites: Least-squares regression [1], Sauer and Schoutens PPG [2], Least-squares regression for vertical displacements [3]	18
14. Near-source peak vertical acceleration contours (in g) for a 15T TNT equivalent surface explosion at J5	21
15. Near-source peak horizontal acceleration contours (in g) for a 15T TNT equivalent surface explosion at J5	22
16. Near-source peak vertical acceleration contours (in g) for a 50T TNT equivalent surface explosion at the proposed LARC	23
17. Near-source peak horizontal acceleration contours (in g) for a 50T TNT equivalent surface explosion at the proposed LARC	24
18. Near-source peak vertical velocity (horizontal velocity, $v_h = 0.5 v_v$) contours (in fps) for a 15T TNT equivalent surface explosion at J5	25
19. Near-source peak vertical velocity (horizontal velocity, $v_h = 0.5 v_v$) contours in fps) for a 50T TNT equivalent surface explosion at the proposed LARC	26
20. Near-source peak vertical or horizontal displacement contours (in in.) for a 15T TNT equivalent surface explosion at J5	27
21. Near-source peak vertical or horizontal displacement contours (in in.) for a 50T TNT equivalent surface explosion at the proposed LARC	28
22. Average damage versus intensity (MMI) for ten construction types ⁹	30
23. Modified Mercalli Intensity (MMI) relationship to peak ground acceleration ⁹	31
24. Accelerations, DISTANT PLAIN 3 (20T TNT equivalent surface blast)	32
25. Velocities, DISTANT PLAIN 3 (20T TNT equivalent surface blast)	33

List of Tables

1. Surface burst close-in peak DI/CI parameters. ⁶	8
2. Surface burst peak ground roll parameters. ⁶	9
3. 15T TNT equivalent explosion at J5	19
4. 50T TNT equivalent explosion at LARC	20
5. Near-surface peak acceleration or velocity magnitudes and duration of the ground motions for DISTANT PLAIN Events referenced	34
6. Trifunac and Brady 50 percent confidence level correlation of peak horizontal velocity to Modified Mercalli Intensity (MMI) for a stiff soil site.	34

Empirical Development of Ground Acceleration, Velocity, and Displacement for Accidental Explosions at J5 or the Proposed Large Altitude Rocket Cell at Arnold Engineering Development Center

Abstract

This study is an assessment of the ground shock which may be generated in the event of an accidental explosion at J5 or the Proposed Large Altitude Rocket Cell (LARC) at the Arnold Engineering Development Center (AEDC). The assessment is accomplished by reviewing existing empirical relationships for predicting ground motion from ground shock. These relationships are compared with data for surface explosions at sites with similar geology and with yields similar to expected conditions at AEDC. Empirical relationships are developed from these data and a judgment made whether to use existing empirical relationships or the relationships developed in this study.

An existing relationship (Lipner et al.) is used to predict velocity; the empirical relationships developed in the course of this study are used to predict acceleration and displacement. The ground motions are presented in table form and as contour plots. Included also is a discussion of damage criteria from blast and earthquake studies.

This report recommends using velocity rather than acceleration as an indicator of structural blast damage. It is recommended that $v = 2$ ips ($v = .167$ fps) be used as the damage threshold value (no major damage for $v \leq 2$ ips).

Introduction

The purpose of this study is to determine the effects of ground shock in the event of an accidental explosion at the proposed Large Altitude Rocket Cell (LARC) or the existing J5 rocket development test cell on the Arnold Engineering Development Center (AEDC), Arnold Air Force Station, Tennessee. An aerial photograph of AEDC is shown in Fig. 1. An accidental explosion of up to 100,000-lbm (50T) TNT equivalent could occur at the proposed LARC, or an accidental explosion of up to 30,000-lbm (15T) TNT equivalent could occur at the existing J5 rocket development test cell.

The results of this study will be used by Structural Mechanics Associates (SMA), of Newport Beach, California, to provide adequate tie-down and lateral-force design requirements for structures and also design data for buried and aboveground piping and ducting.

The effects of high explosive (HE) induced ground shock and of nuclear explosion (NE) induced ground shock have been studied in terms of craters, air slap, blast efficiency, blast geometry, ground layering, ground material, geometry of structures, fragment generation, and a number of other ways. Some studies led to the development of sophisticated computer models, others to empirical methodology. This study identifies existing empirical methodology and compares it with specific explosive events. These events have geology and blast geometry comparable to conditions at the proposed LARC site or the existing J5.

Major uncertainties (site properties, test and analysis data base, scaling of data base to other geologies, blast size, etc.) exist and, where appropriate, are discussed.

Site Description

The site information was provided by E. M. Caldwell at AEDC and J. Kent Lominac, Area En-

gineer with the U.S. Army Corps of Engineers. Caldwell furnished the surface information by

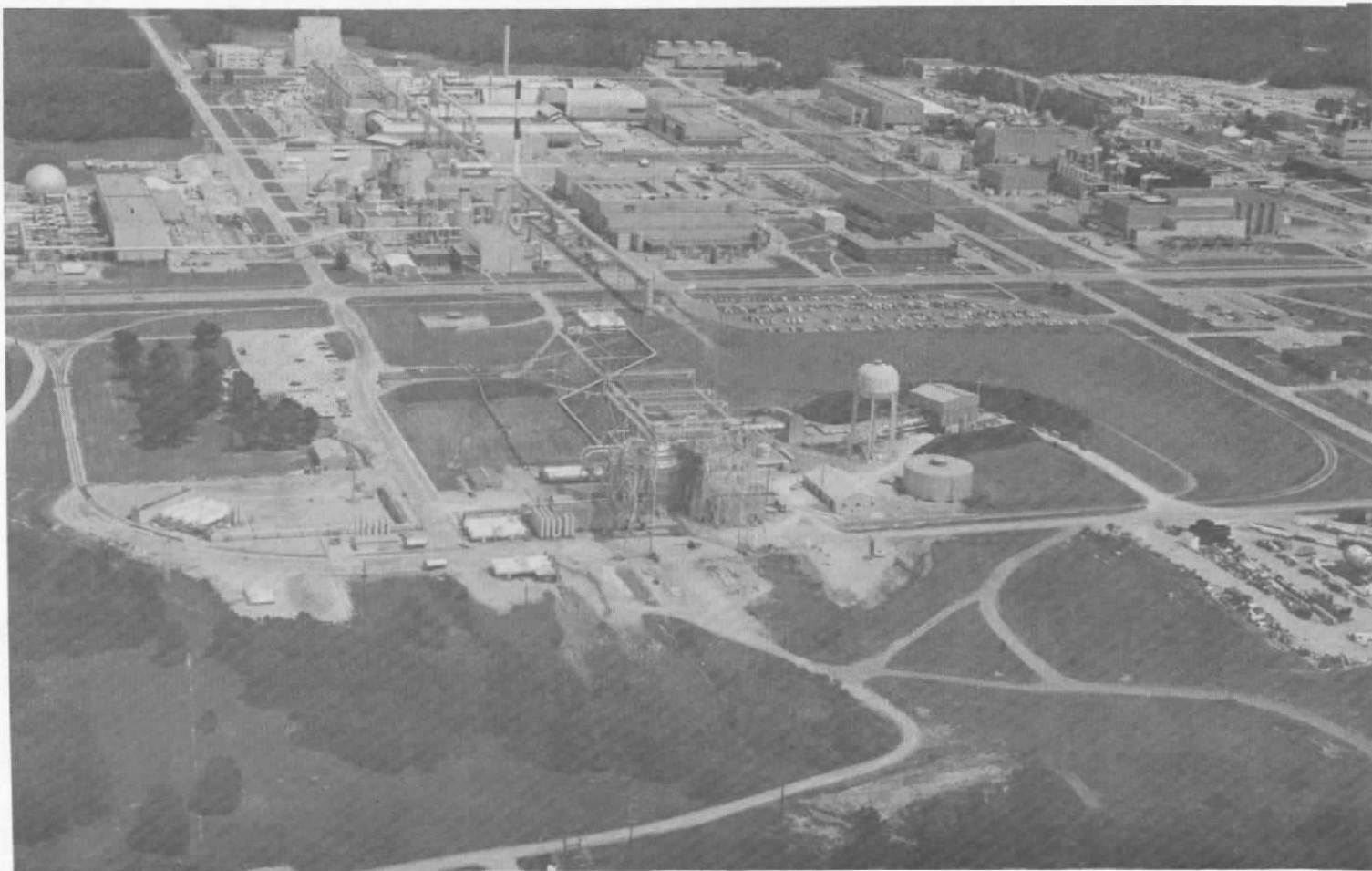


Figure 1. The AEDC Complex.

making available the USDA Soil Survey for Coffee County, Tennessee. Lominac furnished the subsurface information by making available various soil-boring investigations conducted by the U.S. Army Corps of Engineers and Dames & Moore.

Arnold Air Force Station is in south-central Tennessee, approximately 70 miles southeast of Nashville. The site for the proposed LARC facility at AEDC is located on the northeast side of the Retention Reservoir, about one-half mile northwest of the J4 and J5 rocket development test cells¹ and approximately one mile northwest of the Aeropropulsion Systems Test Facility (Fig. 2).

Geologically, AEDC is located in the Highland Rim Physiographic Province near the drainage divide of the Duck and Elk Rivers. West of the site is the Central Basin; east of the site is the transition to the Cumberland Plateau, which is followed by the Valley, the Ridge, and the Blue Ridge Provinces.

Surface elevations range from about 960 feet to 1200 feet. AEDC is at approximately 1100 feet elevation.

The overburden at the site is primarily limestone/dolomite residual material formed by weathering of in situ bedrock. The soil can contain large amounts of residual chert, occurring as angular blocks and fragments. The U.S. Army Corps of Engineers soil-boring investigations indicate that the chert can be so concentrated as to be mistaken for bedrock. The overburden also contains sand, gravel, and silt mixtures.

The first sound rock occurs at a fairly uniform elevation ranging from 1038 to 1043 feet. Approximately 28 feet of hard, dense, light gray, massive, siliceous limestone exists, containing some cavities filled with calcite crystals. The limestone has tested out sound and unweathered except for approximately horizontal bedding planes in the first 5 to 15 feet. These planes, or seams, vary in thickness from 2 to 18 inches; they are evidenced by leaching and solution oxidation discoloration.

Below the limestone, a 19- to 21-foot-thick shale formation occurs (Chattanooga Shale) at a fairly uniform elevation ranging from 1011 to 1014 feet. The shale is hard, dense, black, and cemented. It appears to be extremely fissile at the top and fairly thick-bedded at the bottom.

Underlying the shale is a shaley limestone, identified as the Catheys Formation of the Trenton Group. This shaley limestone is hard, dense, and light-to-dark mottled gray in color.

A static groundwater level has been measured at 6 to 18 feet below ground surface. Dames & Moore of Atlanta reported that the near-surface groundwater resulted from a combination of shallow water conditions, perched water, leakage from underlying artesian aquifers, and surface accumulation. Groundwater investigations carried out by the U.S. Army Corps of Engineers identified the pervious zone at the top of the first sound rock as an artesian aquifer.

Surface Burst Ground Shock Phenomenology

Explosive detonations produce motions and stresses in the earth's surface. These motions and stresses are collectively called ground shock. The ground shock induced by explosive detonations depends on the explosive type, design and yield, the height or depth of burst (HOB), and site characteristics. Three general types of ground shock have been defined²:

Airblast-Induced (AI) Ground Shock: The ground stresses and motions caused by the propagating airblast. Airblast-induced ground shock generally produces the high-frequency components of the motions.

Direct-Induced (DI) Ground Shock: The ground stresses and motions caused by

the initial stress wave from the energy coupled at the burst point in near-surface and underground detonations.

Crater-Induced (CI) Ground Shock: The late-time ground stresses and motions produced by crater formation in a cratering detonation.

For a surface burst, the phenomenology at early-time is dominated by airblast effects. The airblast arrives first, causing air slap on the ground surface. This produces strong downward and outward motions. Compressional motions follow and are associated with the DI/CI ground shock. These compressional motions are a dominant late-time phenomena, producing large upward and outward low-frequency ground motion.

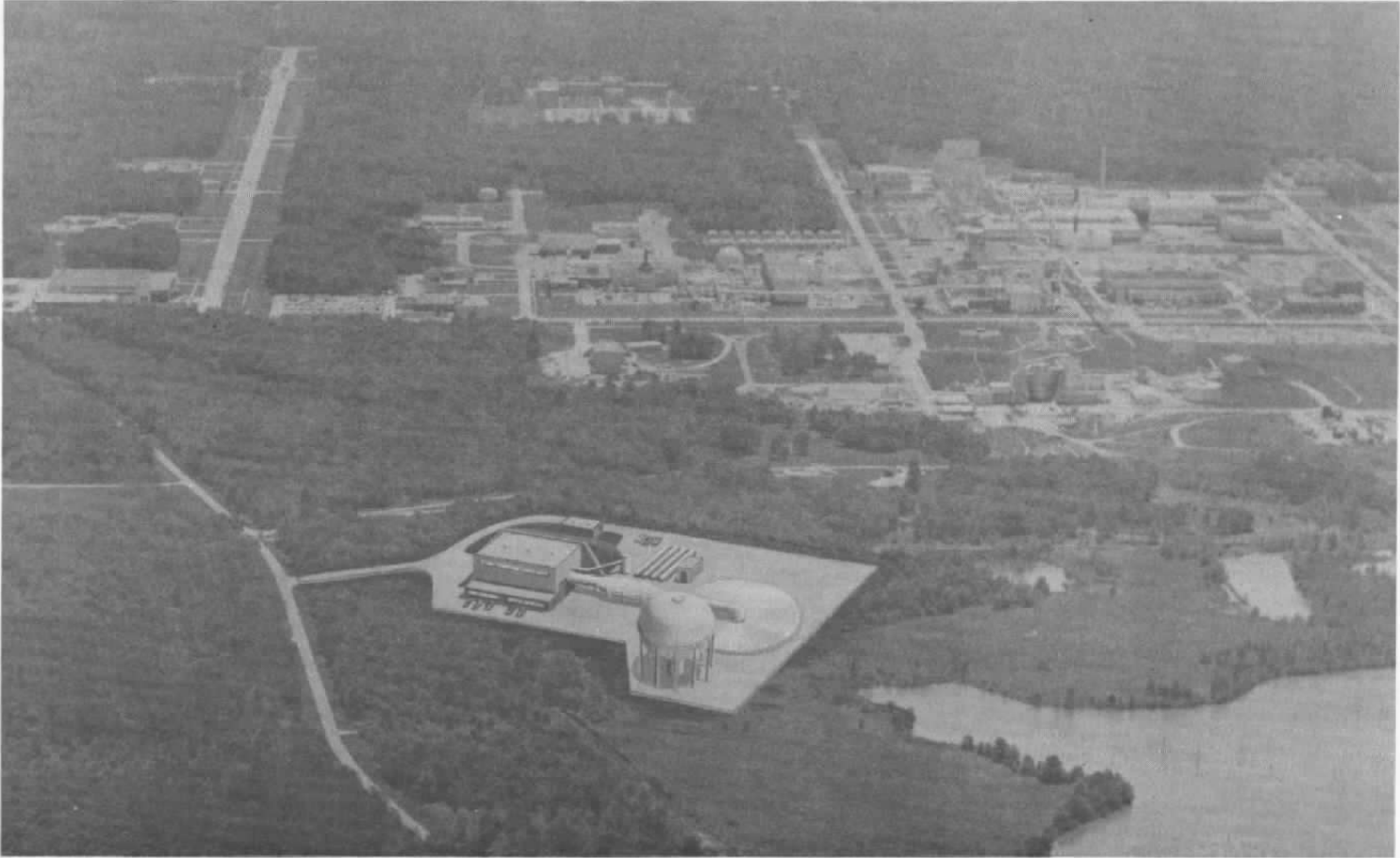


Figure 2. Site for the proposed LARC facility at AEDC.

The range and magnitude of the AI or DI/CI ground motions are dependent on the yield, HOB, and site conditions. It should be noted that, close-in and at early time, ground motion will be AI or DI/CI, but generally not both.

With increasing range from the burst point, the relatively simple motions become a complex wavetrain of surface waves. These surface waves appear to be relatively insensitive to blast geometry. As the horizontal distance from detonation increases, the complex wavetrain of surface waves is similar for a buried cratering burst, for a surface burst, or for an air burst.

Ground-energy coupling is dependent on several factors beside yield, of which the most significant are blast design characteristics, HOB, and site properties. Blast design characteristics include blast source concentration (spherical/point source, directed source, line source, etc.) and type of blast. The design of the blast source (i.e., concentration) aids in directing the energy. The type of blast also affects ground-energy coupling. High explosive sources (TNT, PETN, PBX, etc.) have been found to be approximately twice as efficient as a nuclear source in generating airblast; conventional explosives convert most of the energy into blast and shock while a nuclear source expends a portion of its energy thermally.

The effect of HOB is a major contributor in ground-energy coupling. As HOB increases, AI effects become more dominant, with DI/CI effects diminishing. In general, as HOB increases and AI effects dominate, the close-in early-time ground motion is maximum in the vertical direction. Alternately, as DI/CI effects dominate, the close-in early-time ground motion is maximum in the horizontal direction.

Because many site property effects influence ground-energy coupling, these effects can only be broadly generalized. For nonhomogeneous geological layering, stiffer layers transmit shock faster. Thus, ground shock in a stiffer layer at depth can outrun the airblast conditions still in existence near the surface. Layering and stiffness can also have the effect of strengthening ground shock by wave reflection.

As indicated, the ground shock will be a result of either AI or DI/CI effects and can be broken down into three regions of disturbance types: superseismic, transeismic, and subseismic.³

Media, such as soil, rock, and water, propagate wave disturbances at velocities that are functions of the material properties. At the ground surface, three types of wave disturbance produce the majority of the ground motion; they are identified

as primary (p), secondary (s), and Rayleigh waves. The p- and s-waves are also known as body waves and are, respectively, compressional and shear in nature. Rayleigh waves are also known as surface waves. The presence of all three waves is not limited to the surface, but the Rayleigh wave attenuates rapidly with depth. Flint and Skinner further describe the manner in which these waves deform solids.⁴ The speeds of propagation (C) of these waves are related as follows:

$$C_p > C_s > C_R,$$

where C_p is the p-wave propagation velocity, C_s is the s-wave propagation velocity, and C_R is the Rayleigh wave propagation velocity. The above relationship indicates a point at or just beneath the surface is first affected by the p-wave arrival, second by s-wave arrival, and finally by arrival of the Rayleigh wave. At the surface, the p- and s-waves decay faster with range than does the Rayleigh wave.

The superseismic region is defined as that region where airblast velocity exceeds all wave propagation velocities:

$$U > C_p > C_s,$$

where U is the airblast velocity. Since U is larger than C_p or C_s , no disturbance exists ahead of the airblast, and ground shock trails airblast.

When airblast shock velocity falls below the p-wave propagation velocity but still exceeds the s-wave propagation, the region is known as transeismic. In this region, compressional disturbances can propagate in the ground ahead of the airblast:

$$C_p > U > C_s,$$

When airblast velocity falls below the s-wave propagation, the subseismic case exists:

$$C_p > C_s > U.$$

For both transeismic and subseismic regions, compressional and shear disturbances can propagate through the ground ahead of the airblast shock. For that reason, they are often collectively referred to as the *outrunning region* to indicate that ground shock has outrun the airblast shock.

Several factors can influence or contribute to the complex nature of the surface waves at early- or late-time. One result of such influence or contribution could be refracted and reflected waves

outrunning airblast shock when superseismic conditions would otherwise exist at the surface. Another could be the existence of superseismic con-

ditions when outrunning conditions would otherwise exist at the surface.

Study Methodology

Competent ground shock prediction for a site can be obtained through use of large-scale computer code modeling techniques. Simplified techniques are available⁵ but have large uncertainties associated with them. Most of the techniques are based on some combination of data from theoretical studies and field test observations. These techniques approximate the complete environment that will result from disturbances arriving from all sources by superimposing air detonation, surface detonation, and contained detonation motion according to their relative time-phasing.

For this study, appropriate surface explosion methodology is identified and used to predict ground motions at AEDC for an accidental explosion in the J5 and in the proposed LARC rocket development test cells. For such an explosion, it is believed that most of the energy will be directly coupled with the ground (i.e., most of the airblast will be contained). The predicted motions are compared with measured ground motions for events similar in yield and site conditions. A judgment is then made as to which procedure makes the best prediction of ground motions.

Lipner et al.⁶ used a ground shock data base gathered from nuclear and high explosive test results. They used the data base to generate ground motion predictions for surface burst air slap, surface burst close-in DI/CI, and surface burst ground roll conditions. For each surface burst condition, four generic site types are defined: (a) dry soil-seismic velocity less than 3,000 fps, (b) wet soil-seismic velocity between 3,000 and 6,000 fps, (c) dry soft rock-seismic velocity between 6,000 and 12,000 fps, and (d) hard rock-seismic velocity greater than 12,000 fps. Parameters are defined for each generic site category with each surface burst condition.

A recommended weighting factor of 2.0 can be applied to the equivalent TNT yield.² This weighting is recommended when blast wave strengthening is expected from ground reflection. The site conditions at AEDC (stiffer soils with near-surface ground water table [GWT]) are such that blast wave strengthening may exist.

The generic wet site surface burst close-in DI/CI and surface burst ground roll relationships

for conditions at AEDC are shown in Figs. 3-7. Ground roll is the name given by Lipner et al. to ground motion found in the outrunning region. Figures 4 and 5 show that, for AEDC, the generic relationships indicate that ground roll will dominate acceleration and velocity at ranges of 40 feet and greater for both yield sizes.

Figures 6 and 7 indicate that ground roll displacement will dominate at ranges of 200 feet and greater for both yield sizes. The equivalent yield scaling relation for DI/CI velocity and displacement has not been demonstrated to be consistent (DI/CI velocity and displacement are more consistent when scaled to crater volume) and may have a high uncertainty associated with the predicted values. This is particularly true for displacements where the data base has been generated from integrated acceleration and/or velocity time histories.

The acceleration relationship in Fig. 3 is taken from Crawford et al.² and from Newmark and Halmiwanger,⁷ who specify:

$$a = a_0(W/1 \text{ MT})(R/1000 \text{ ft})^{-4}, \quad (1)$$

for all ranges, where the acceleration correction factor, a_0 , is 140 g for hard rock, 25 g for soft rock, and 5 g for dry soil; the explosive force, W , is in megatons (MT); and the distance from the explosive source, R , is in feet. Lipner et al. used a value of a_0 for wet soil between that for soft rock and dry soil. They found the relationship to be very conservative in estimating acceleration. In the ground roll region, they subscribe to the usual practice of equating vertical and horizontal acceleration. The relevant surface burst conditions from Lipner et al. are given in Tables 1 and 2.

Sauer and Schoutens³ use a ground shock data base derived from nuclear explosive tests at the Nevada Test Site (NTS) and the Pacific Proving Ground (PPG). The outrunning acceleration relationships developed from the PPG data are as follows:

$$a_v = 2 \times 10^{10}(R/W^{1/3})^{-3.5} \quad (2) \\ \text{for } 150 \leq (R/W^{1/3}) \leq 800,$$

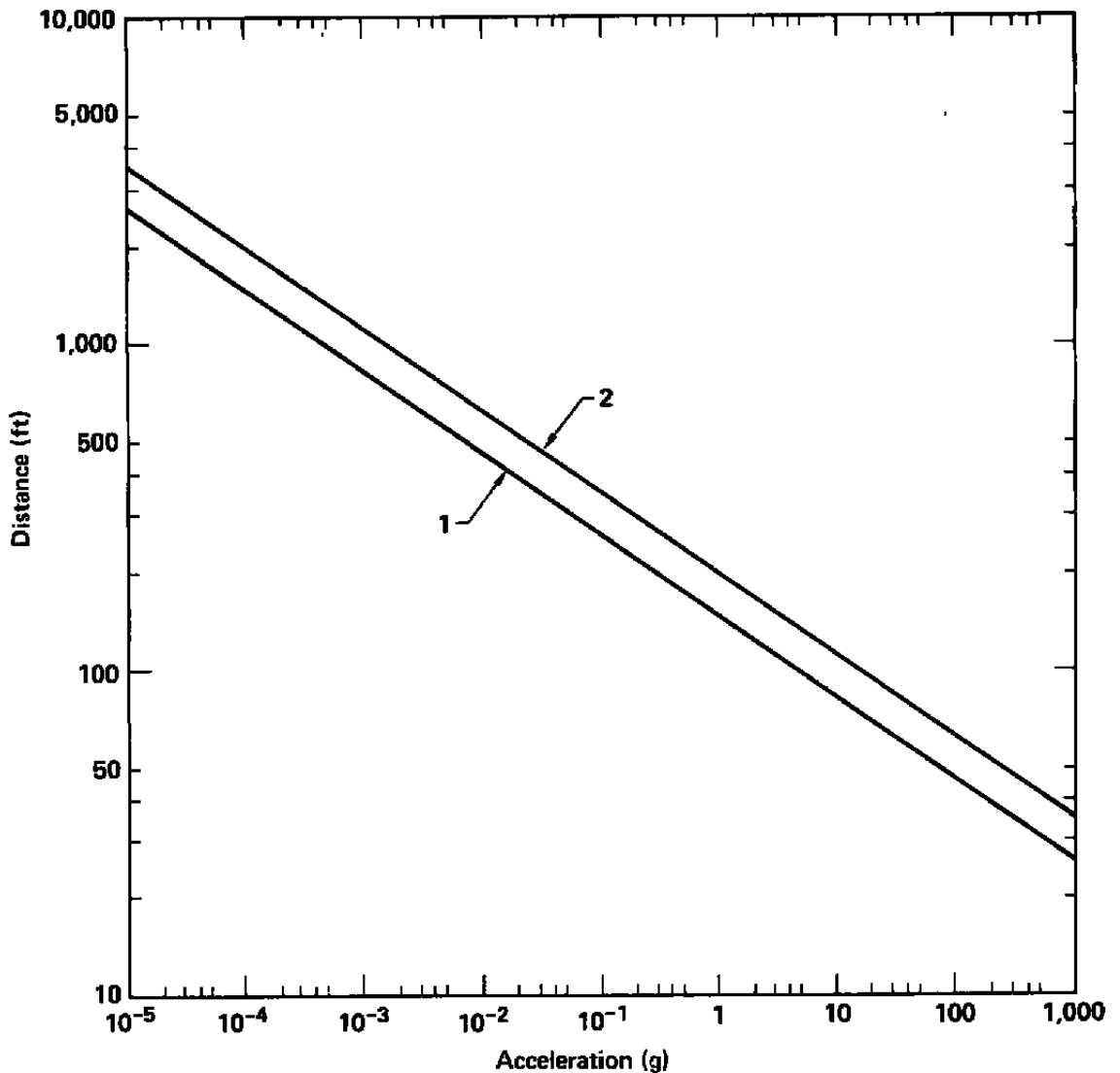


Figure 3. 15T [1] and 50T [2] equivalent (2.0 weighting factor) surface burst close-in peak DI/CI acceleration for generic wet site.

$$a_v = 1 \times 10^6 (R/W^{1/3})^{-2} \quad (3)$$

for $800 < (R/W^{1/3}) \leq 3000$,

where W is in kilotons, R is the ground range in feet, and a_v is the maximum vertical acceleration in g. The associated error range is +200%, -70%. The NTS data have the following relationship:

$$a_v = 17.5 \times 10^6 (R/W^{1/3})^{-2} \quad (4)$$

for $800 \leq (R/W^{1/3}) \leq 3000$,

where values and the associated error are as defined previously. The NTS data are asymptotic to the defined relationship but fall far below it in the scaled region less than 800 [$(R/W^{1/3}) < 800$]. Sauer and Schoutens suggest that horizontal acceleration should also be taken as equal to vertical in the outrunning region. It is only in the superseismic region that horizontal values are suggested to be significantly below vertical values. For that region, they suggest horizontal values of 0.2 to 0.5 times the vertical accelerations.

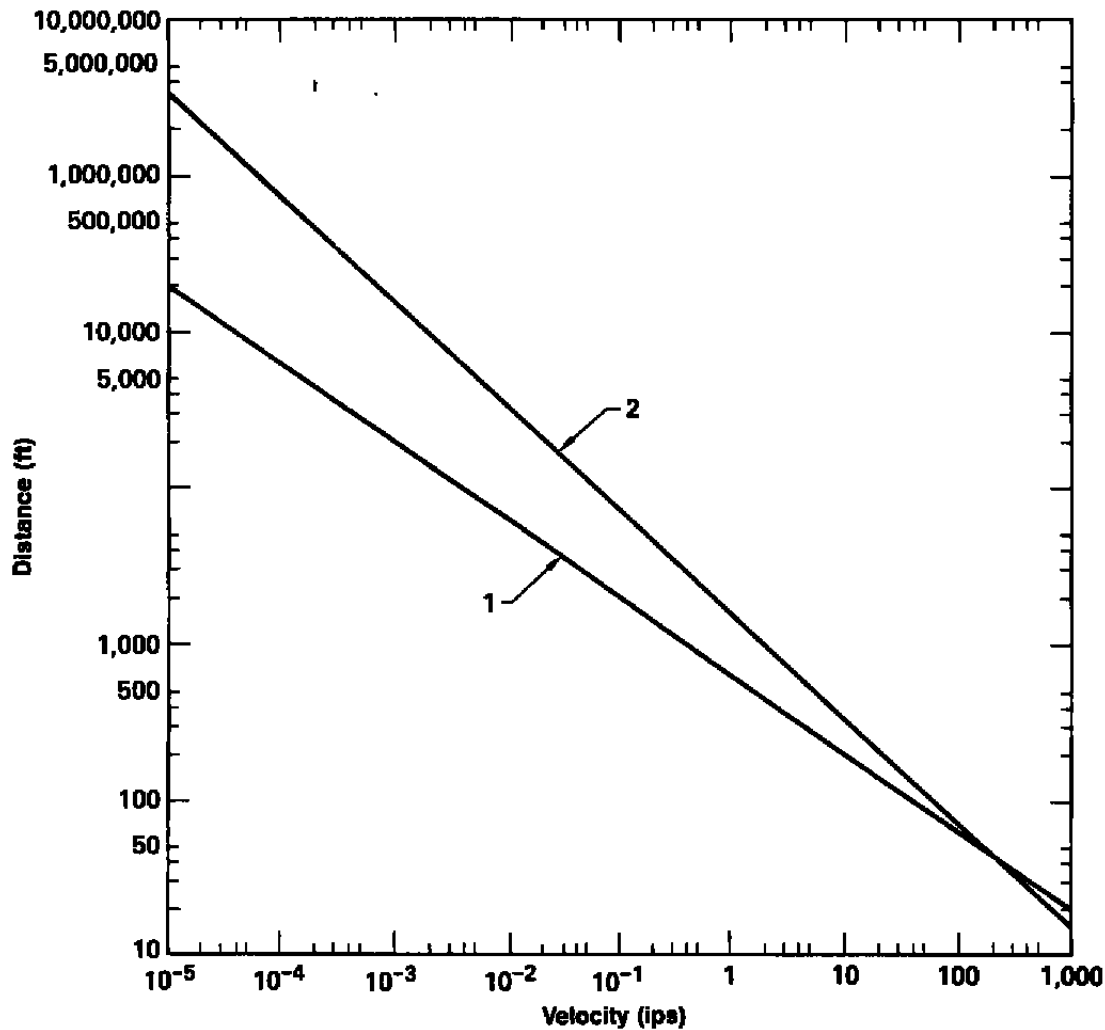


Figure 4. 50T TNT equivalent (2.0 weighting factor) surface burst peak DI/CI velocity [1] and peak ground roll velocity [2] for generic wet site.

Table 1. Surface burst close-in peak DI/CI parameters.⁶

Environment parameter	Reference value				Scaling factors		2σ uncertainty factor
	Dry soil	Wet soil	Soft rock	Hard rock	A	B	
	Environment Value = (Reference Value)(W/1 MT) ^{1/3} (1000 ft/R) ³						
Crater volume (10 ⁶ ft ³)	50	170	40	30	1	0	1.8
Displacement (in.)	100	510	75	50	4/3	3	3.5
Velocity (ips)	50	180	110	150	2/3	2	3.5
Acceleration (g)	5	15	25	140	1	4	5
Stress (psf)	75	750	880	5000	2/3	2	4

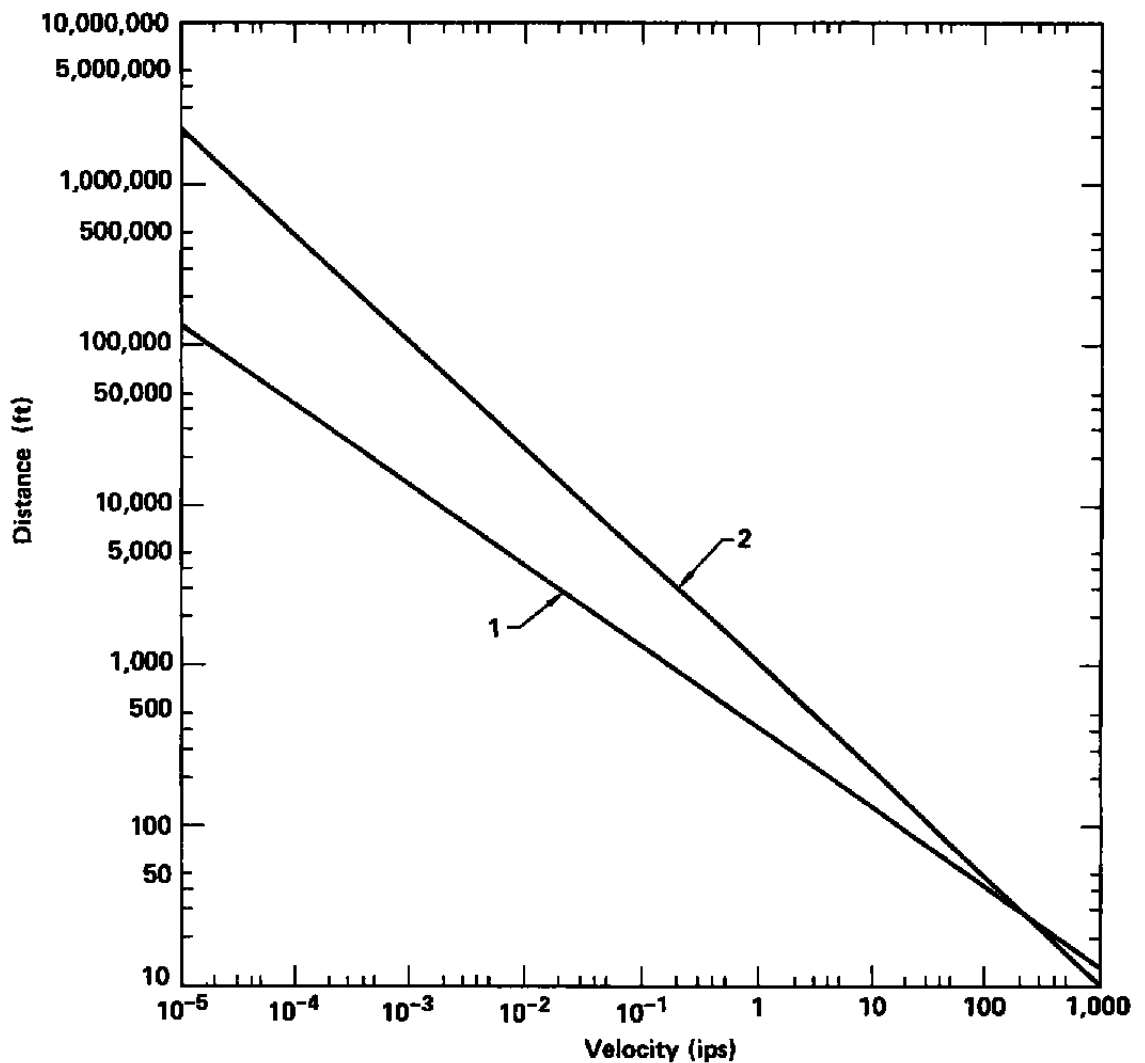


Figure 5. 15T TNT equivalent (2.0 weighting factor) surface burst peak DI/CI velocity [1] and peak ground roll velocity [2] for generic wet site.

Table 2. Surface burst peak ground roll parameters.⁶

<i>Environment Value = (Reference Value)(W/1 MT)⁴(10,000 ft/R)⁸</i>							
Prediction parameter	Environment parameter	Generic site				Scaling factors	
		Dry soil	Wet soil	Soft rock	Hard rock	A	B
Reference value	Displacement (in.)	1.5	1.5	0.6	0.6	2/3	1
	Velocity (ips)	6.0	6.0	2.4	2.4	1/2	3/2
2σ uncertainty factor	Displacement	3.5	4.0	5.0	5.0	—	—
	Velocity	3.5	3.5	4.0	4.0	—	—

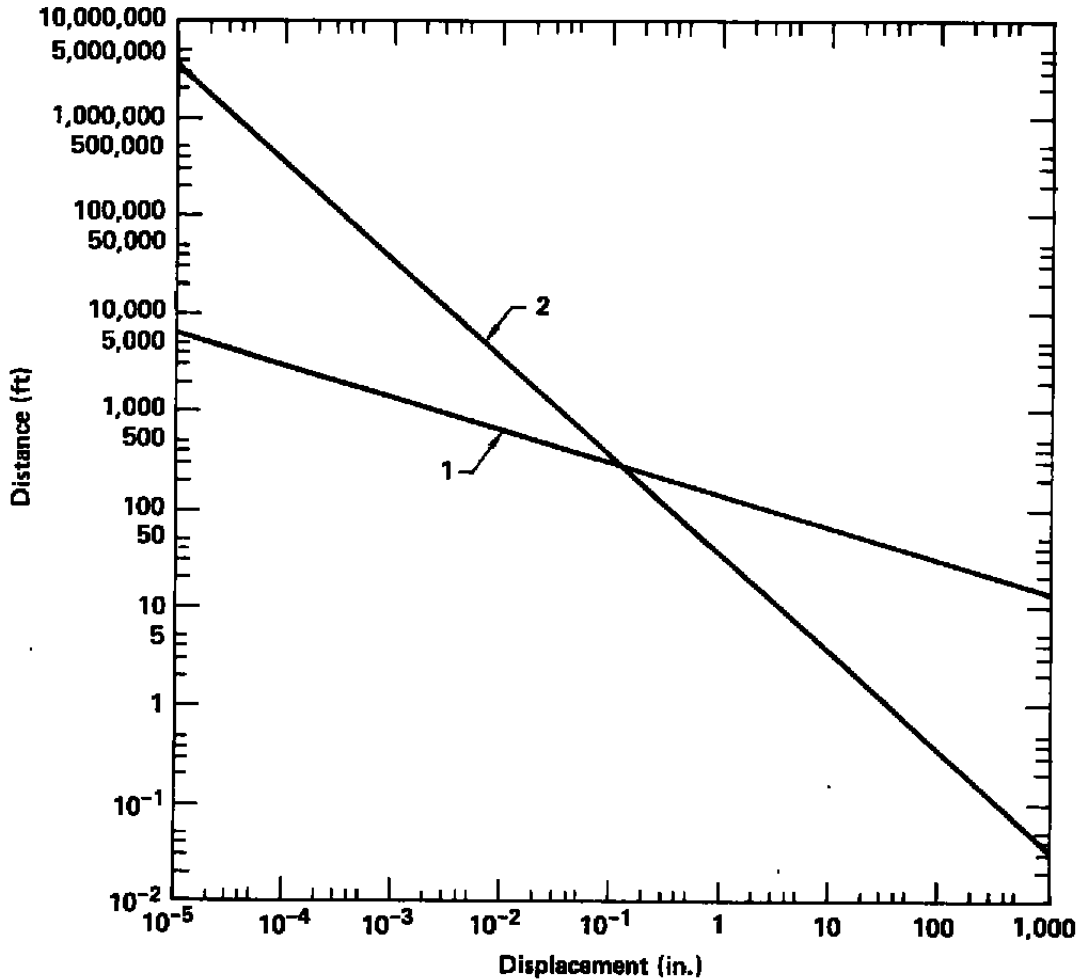


Figure 6. 50T TNT equivalent surface burst peak DI/CI displacement [1] and peak ground roll displacement [2] for generic wet site.

Sauer and Schouten present the following correlations for maximum vertical velocity in the outrunning region:

for NTS,

$$v_v = 2 \times 10^8 (R/W^{1/3})^{-2} \quad (5)$$

for PPG,

$$v_v = 5 \times 10^7 (R/W^{1/3})^{-2} \quad (6)$$

where v_v is in fps, R is in feet, and W is in megatons. Sauer recommends that the maximum horizontal velocity be taken as 0.25 to 0.5 of the maximum vertical velocity in the outrunning region.

Displacement in the superseismic region is predicted by various models which correlate air slap overpressure to maximum displacement. In the outrunning region, Sauer and Schoutens found that an inverse-square law attenuation with ground range fit their PPG data, although the scatter was quite large. They also found that horizontal displacements appear to be approximately equal to vertical displacements. The Sauer and Schoutens PPG displacement relationship is:

$$d_{\max}/W^{1/3} = 7600(R/W^{1/3})^{-2}, \quad (7)$$

where d_{\max} and R are in feet and W is in kilotons.

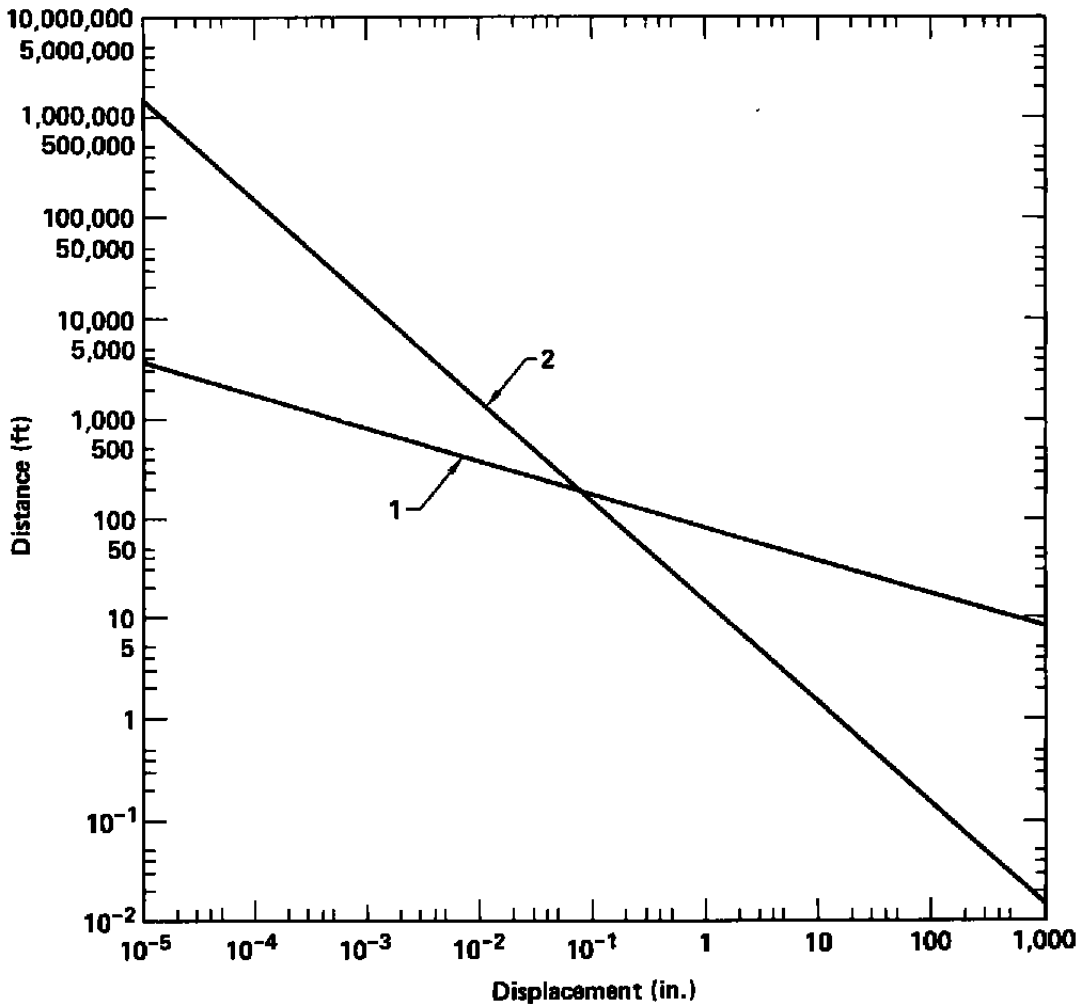


Figure 7. 15T TNT equivalent surface burst peak DI/CI displacement [1] and peak ground roll displacement [2] for generic wet site.

Comparison of Predicted Values to Specific Sites

AEDC has a general site condition of approximately 80 feet of wet (GWT at about 12 feet), layered soil made up of clays, silts, and sands overlying limestone/dolomite. Two event series have similar test media: DISTANT PLAIN and MIDDLE GUST.

Most event data lack acceleration and displacement measurements. Some studies have calculated accelerations, where maximum vertical downward acceleration is related to the shape of the rise time to the maximum velocity. At the ground surface, the rise is equal to the rise time of

the airblast. A rise time relationship can also be used that considers the wave propagation velocity of the media and their seismic in situ velocity. Near-surface maximum displacements are found from integrated near-surface velocity time histories.

Acceleration Comparisons

Acceleration data, as indicated, are not as widely available as velocity data. Of the six events

referenced for velocity data, only three had acceleration data (DISTANT PLAIN 2A, 3, and 5). The acceleration data for these events are shown in Figs. 8 and 9, along with the data for DISTANT PLAIN 4 (a 50T TNT equivalent yield event). The generic acceleration relationship [Eq. (1)] and the Sauer and Schoutens outrunning acceleration relationships for PPG [Eqs. (2) and (3)] and NTS [Eq. (4)], along with a least-squares regression analysis, are plotted for comparison with event data. The least-squares regression analyses give:

$$a_v = 6.7 \times 10^6 (R/W^{1/3})^{-19}, \quad (8)$$

$$a_h = 1.7 \times 10^5 (R/W^{1/3})^{-16}, \quad (9)$$

where W is in kilotons, R is in feet, and a is acceleration in g . The regression analyses give results very similar to the Sauer and Schoutens NTS relationship.

The Sauer and Schoutens NTS relationship seems to fit well with the vertical acceleration data (Fig. 8). According to the Sauer and Schoutens finding, for a 20T TNT equivalent event at NTS, their relationship should highly overpredict accelerations at ranges of less than about 220 feet. But for the DISTANT PLAIN data, the NTS relationship predicts quite well for the range under its expected use (data are asymptotic); the limited data available in the outrunning region indicate the relationship is adequate. No data are available in the range outside the upper limit for the relationship.

The horizontal acceleration data are shown in Fig. 9. The scatter is large, which is typical for maximum horizontal acceleration data. The best correlation, other than the least-squares regression analysis, comes from using one of the Sauer and Schoutens weighting factors for the subseismic region (the $0.2 a_{vmax}$ correlates best). Many experts recommend assuming maximum horizontal and vertical accelerations to be equal in the outrunning region, but this assumption does not appear valid with the data available (NTS peak a_v is shown in Fig. 9 for the outrunning range). Again, no data are available outside the upper end of the NTS relationship range limits, so the assumption is made that it still holds.

No directly measured acceleration data are available for larger yield events on wet, layered sites. Indications are that, in the outrunning region, acceleration is not very sensitive to yield

scaling so the relationships should hold for higher yield events.

The Sauer and Schoutens NTS relationship (with horizontal acceleration correction) or the least-squares regression analyses are suitable for predicting ground acceleration at AEDC. It is felt that the least-squares regression relationships are most appropriate.

Velocity Comparisons

Velocity data for the relevant events are taken from edited peak ground motion data. Some event data are reported as peak horizontal and vertical for varying range and depth; others attempt to report AI velocities separate from DI/CI velocities. For these cases, no vertical component of DI/CI velocities is reported. Since the AI and DI/CI horizontal velocities are approximately equal for these cases, and especially since ground motion in the outrunning region is not source dependent, both surface burst conditions are plotted.

100T TNT Equivalent Yield Events

DISTANT PLAIN 6 and MIDDLE GUST III are 100T TNT equivalent yield events suited for comparison to evaluate ground motion prediction for an accidental explosion at the LARC at AEDC. The near-surface peak velocities are shown in Fig. 10. Four velocity relationships are plotted: the Sauer⁸ using DISTANT PLAIN, PRAIRIE FLAT, and FLAT TOP events; the Lipner et al. generic ground roll wet site (Table 2); the Sauer PPG [Eq. (6)]; and the Sauer NTS [Eq. (5)]. The best fit comes from the generic ground roll relationship with the recommended twice-the-yield weighting factor (curve 2b).

20T TNT Equivalent Yield Events

PLAIN 2A, 3, and 5, along with MIDDLE GUST I, are 20T TNT equivalent yield events which correspond best for comparison purposes to those expected for an accidental explosion in the J5 rocket development test cell at AEDC. The near-surface peak velocities are plotted in Fig. 11. The Lipner et al. ground roll velocity for the generic wet site is plotted, along with the Sauer NTS and PPG velocity relationships. The best fit is the generic ground roll relationship utilizing the twice-the-yield weighting factor (curve 3b).

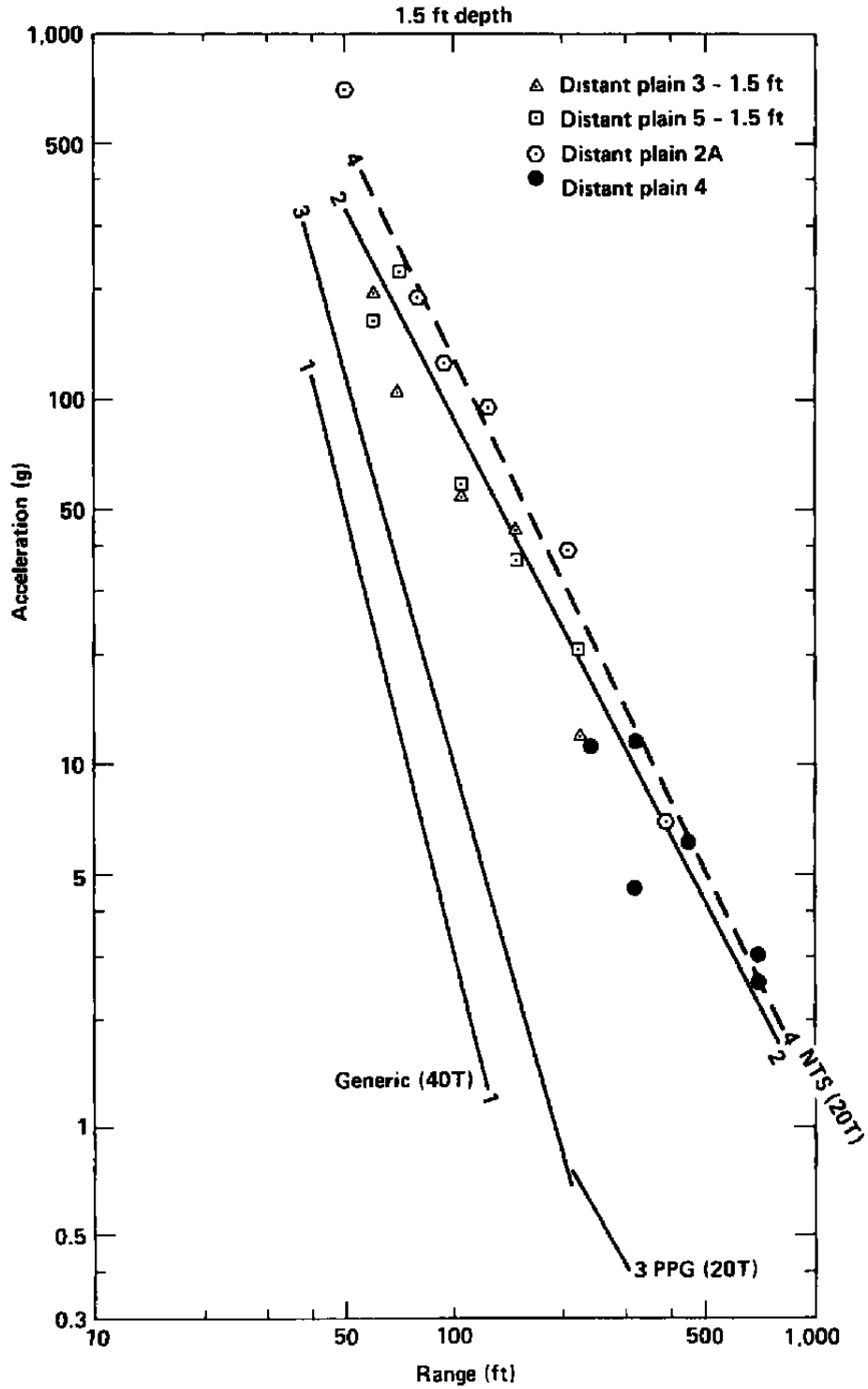


Figure 8. Near-surface peak vertical acceleration for surface and surface-tangent 20T high explosive events at wet, layered sites: Generic w/2.0 yield weighting [1], Least-squares regression [2], Sauer and Schoutens PPG [3], Sauer and Schoutens NTS [4] peak vertical acceleration relationships.

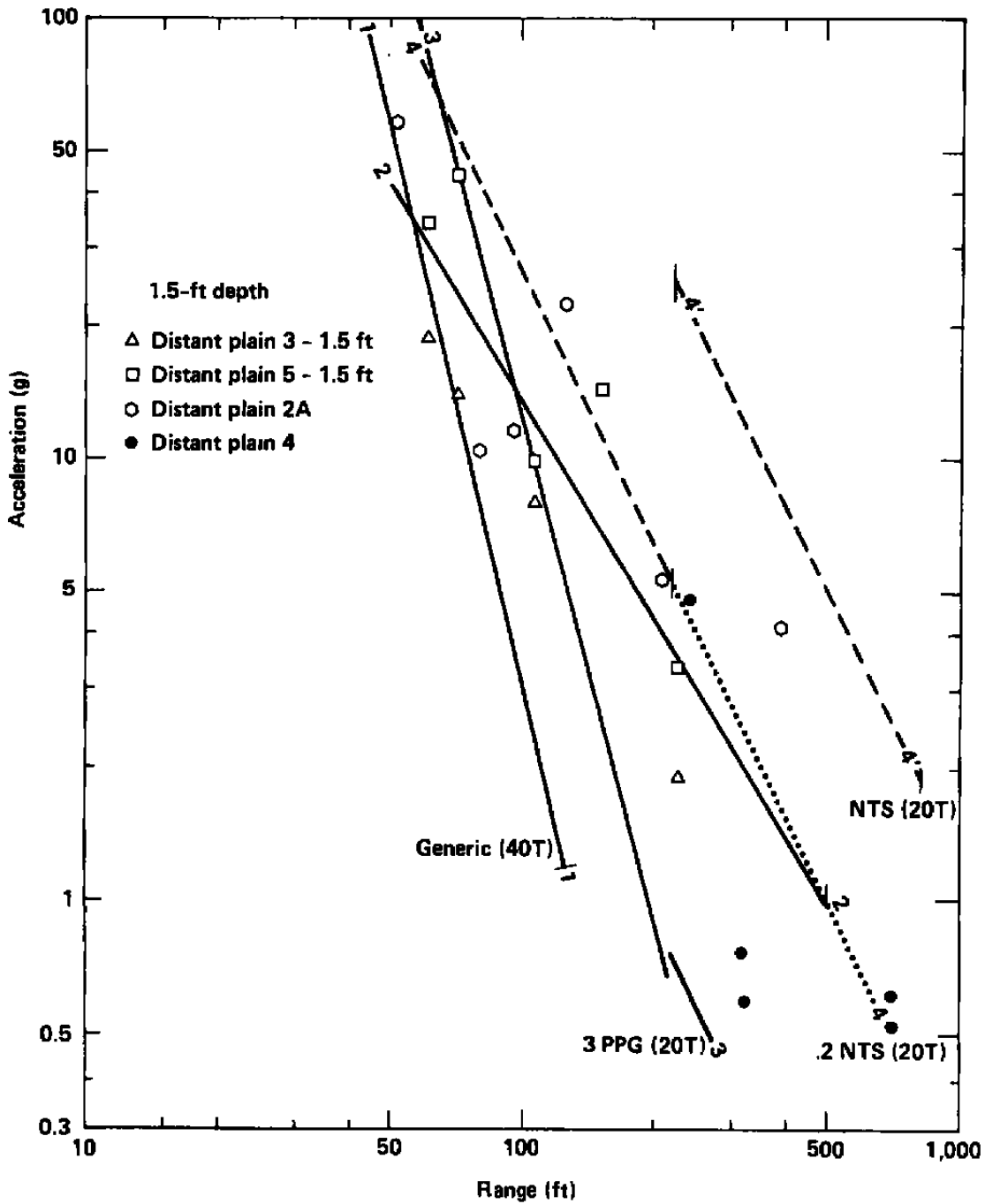


Figure 9. Near-surface peak horizontal acceleration for surface and surface-tangent 20T high explosive events at wet, layered sites: Generic w/2.0 yield weighting [1], Least-squares regression [2], Sauer and Schoutens PPG [3], Sauer and Schoutens NTS [4] peak horizontal acceleration relationships.

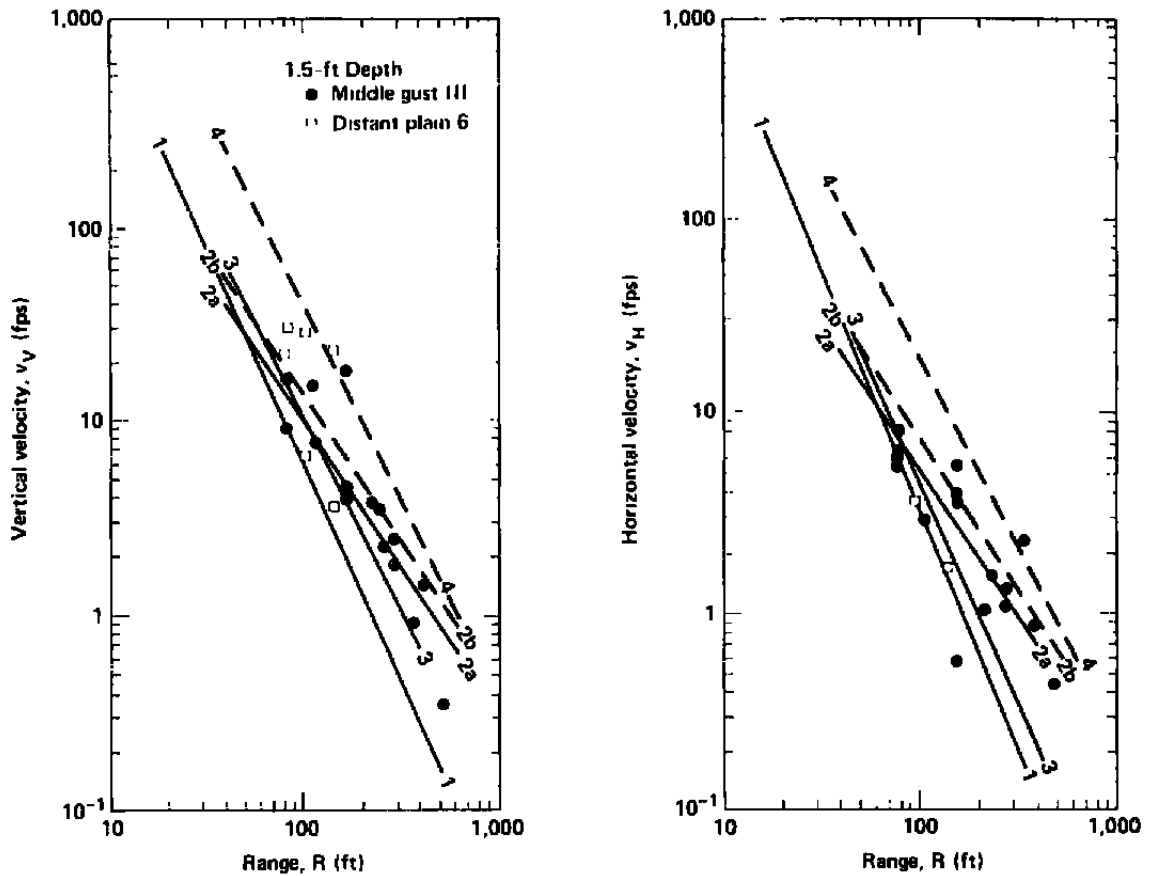


Figure 10. Near-surface peak velocity for surface tangent 100T high explosive events at wet, layered sites: Sauer HE [1], Generic Ground Roll [2a], Generic Ground Roll w/2.0 yield weighting [2b], Sauer PPG [3], Sauer NTS [4] peak velocity relationships.

Displacement Comparisons

Displacement data available are derived from integrated velocity time histories. The displacement data are shown in Figs. 12 and 13. Data from varying size events are plotted together, with yield used to weight the range and displacement. Least-squares regression analyses generate the following relationships:

$$d_{i,max}/W^{1/3} = 2.4 \times 10^6 (R/W^{1/3})^{-3}, \quad (10)$$

$$d_{h,max}/W^{1/3} = 5 \times 10^7 (R/W^{1/3})^{-2.65}, \quad (11)$$

where $d_{i,max}$ and $d_{h,max}$ are in inches, W is in kilotons, and R is in feet. The Sauer and Schoutens PPG displacement relationship [Eq. (7)] is plotted (curve 2) in Figs. 12 and 13; their relationship falls considerably below the data. The generic site relationship is not plotted as it is not compatible with yield weighting. A comparison of the value predicted by the generic site relationship with the data shows that the generic relationship predicts vastly below the data.

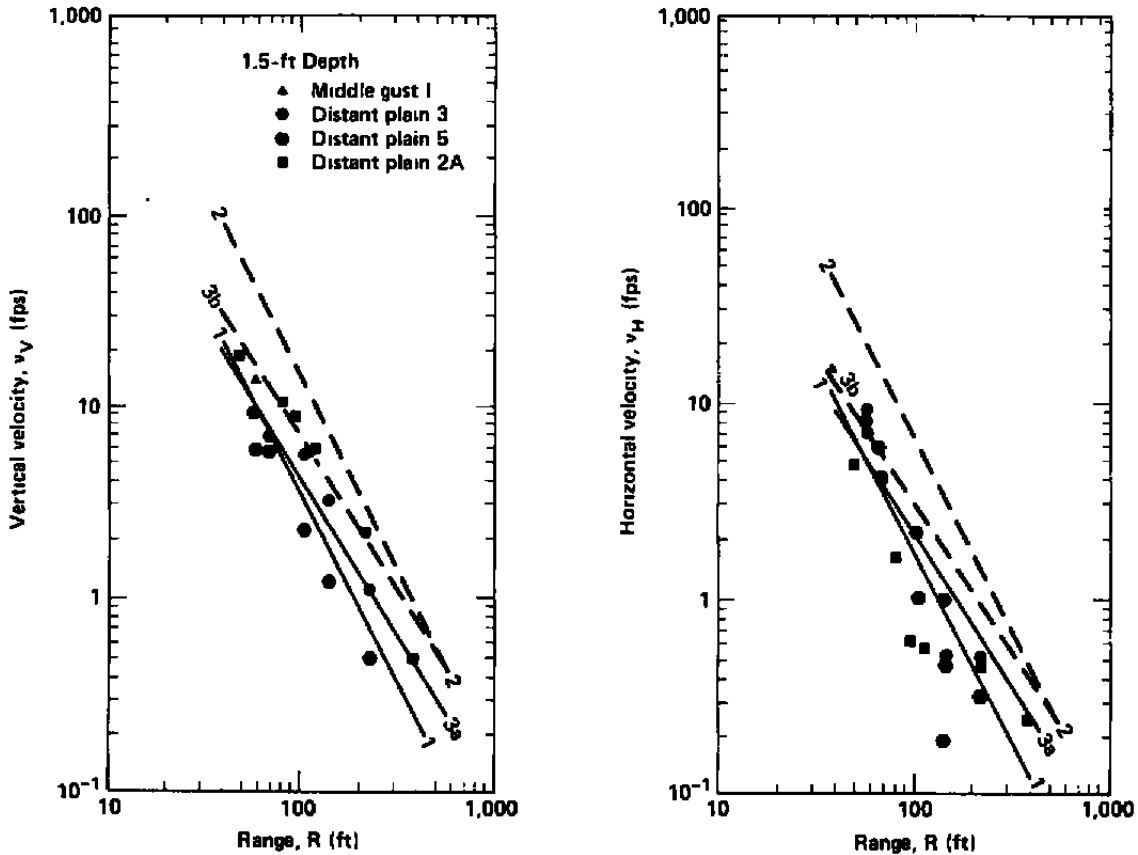


Figure 11. Near-surface peak velocity for surface and surface-tangent 20T high explosive events at wet, layered sites: Sauer PPG [1], Sauer NTS [2], Generic Ground Roll [3a], Generic Ground Roll w/2.0 yield weighting [3b] peak velocity relationships.

The vertical and horizontal displacements derived from the integrated velocity time histories are so similar in magnitude that a single relationship is developed to predict ground displacements at AEDC. That relationship is:

$$d_{max}/W^{1/3} = 1 \times 10^6 (R/W^{1/3})^{-2.8}, \quad (12)$$

where d_{max} is in inches, W is in kilotons, and R is in feet.

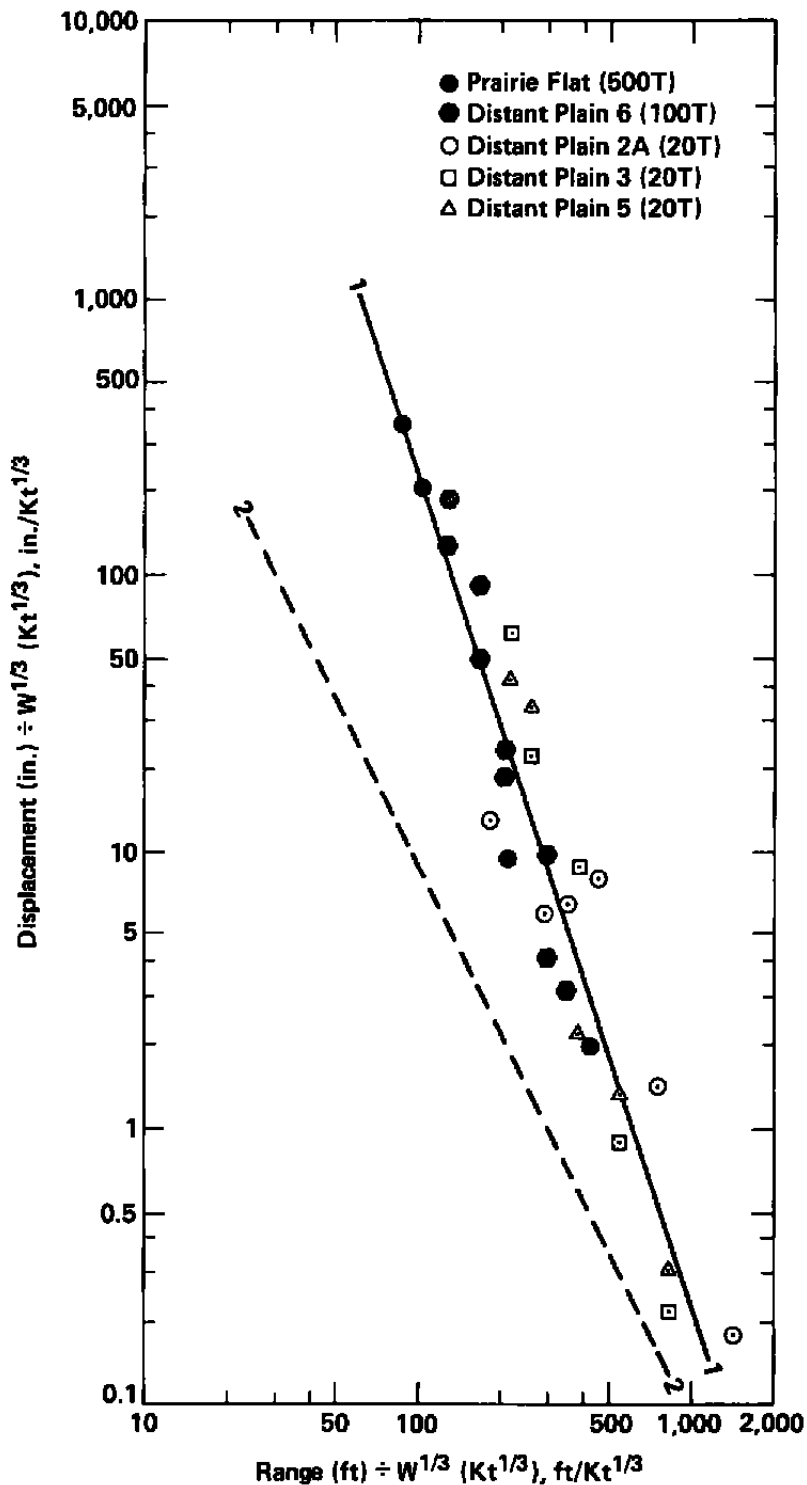


Figure 12. Near-surface peak vertical displacement for high explosive events at wet, layered sites: Least-squares regression [1], Sauer and Schoutens PPG [2].

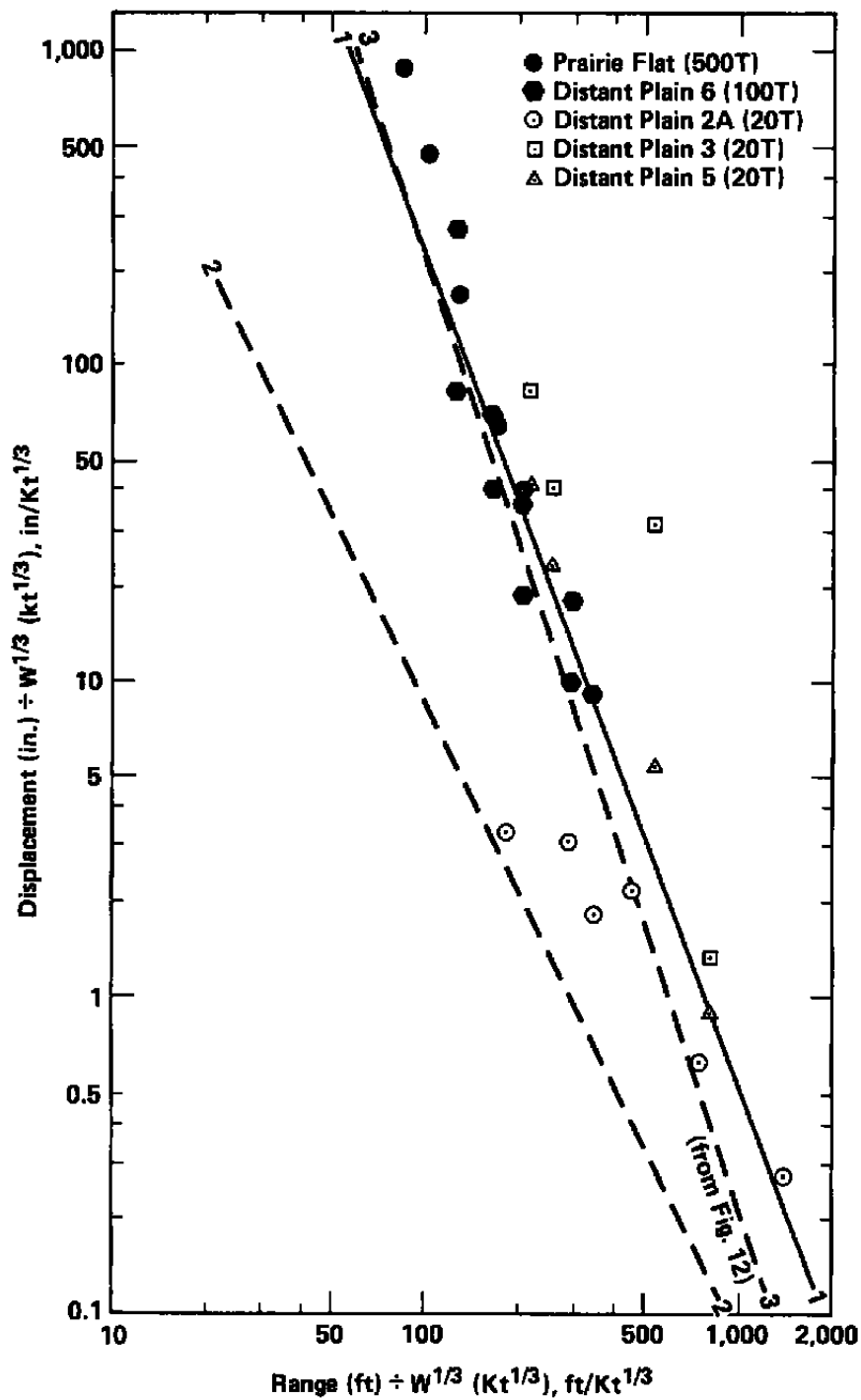


Figure 13. Near-surface peak horizontal displacement for high explosive events at wet, layered sites: Least-squares regression [1], Sauer and Schoutens PPG [2], Least-squares regression for vertical displacements [3].

Results

The near-surface acceleration, velocity, and displacement ground motions for the required yields at specific intervals are listed in Tables 3 and 4, for a 15T and 50T TNT equivalent explosion, respectively. The 15T and 50T TNT equivalent yield acceleration ground motions are based on Eqs. (8) and (9), the velocity ground motions on the Lipner et al. generic wet site relationship on Table 2, and the displacement ground motions on Eq. (12).

These relationships [Eqs. (8), (9), (12), and Table 2] give the best estimate of what will occur

at the near-surface. Unique conditions may exist which will cause values either higher or lower than those predicted (e.g., an extreme yield could result in over-predicted ground motions; highly-directional blast geometry could cause either a reduction or an increase in the vertical component of motion; it is even possible that the cell itself could induce ground-energy coupling to increase the horizontal component). Although such conditions could exist, it is believed that the assumption of best-estimate is valid. And it should be stressed that the equations of motion presented here are

Table 3. 15T TNT equivalent explosion at J5.

a_v	Acceleration (g)		Velocity (fps)			Displacement (in.)		
	Range (ft)	a_h	Range (ft)	v_v	v_h	Range (ft)	d	Range (ft)
300.	48.0	50.	39.7	15.	7.5	51.1	300.	14.0
150.	69.1	25.	61.3	10.	5.0	66.9	150.	18.0
75.	99.5	20.	70.5	5.	2.5	106.3	75.	23.0
50.	123.2	15.	84.3	4.	2.0	123.3	50.	26.6
25.	177.4	10.	108.7	3.	1.5	149.4	25.	34.1
20.	199.5	9.	116.1	2.	1.0	195.7	20.	36.9
15.	232.1	8.	124.9	1.	.5	310.7	15.	40.9
10.	287.3	7.	135.8	.9	.45	333.3	10.	47.3
9.	303.7	6.	149.5	.8	.4	360.6	5.	60.6
8.	323.1	5.	167.6	.7	.35	394.1	4.	65.6
7.	346.7	4.	192.7	.6	.3	436.8	3.	72.7
6.	376.0	3.	230.6	.5	.25	493.2	2.	84.0
5.	413.8	2.	297.1	.4	.2	572.4	1.	107.7
4.	465.4	1.	458.2	.3	.15	693.4	.75	119.3
3.	541.5	.9	489.4	.2	.1	908.6	.5	137.9
2.	670.3	.8	526.8	.15	.075	1100.6	.25	176.6
1.	965.4	.7	572.6	.1	.05	1442.2	.15	212.0
.9	1020.4	.6	630.5	.09	.045	1547.2	.05	313.8
.8	1085.7	.5	706.7	.08	.04	1673.6	.025	402.0
.7	1164.7	.4	812.4	.07	.035	1829.4	.005	714.2
.6	1263.2	.3	972.4	.06	.03	2027.4		
.5	1390.4	.2	1252.9	.05	.025	2289.4		
.4	1563.7	.15	1499.7	.04	.02	2656.6		
.3	1819.3	.1	1932.2	.03	.015	3218.3		
.2	2252.1	.05	2979.9	.02	.01	4217.2		
.15	2620.2			.01	.005	6694.3		
.1	3243.5							
.05	4671.5							

Table 4. 50T TNT equivalent explosion at LARC.

Acceleration (g)				Velocity (fps)			Displacement (in.)	
a_v	Range (ft)	a_h	Range (ft)	v_v	v_h	Range (ft)	d	Range (ft)
300.	71.7	50.	59.4	15.0	7.5	76.3	300.	24.2
150.	103.2	25.	91.5	10.	5.0	100.0	150.	31.0
75.	148.6	20.	105.2	5.	2.5	158.7	75.	39.7
50.	184.0	15.	126.0	4.	2.0	184.2	50.	45.9
25.	265.0	10.	162.3	3.	1.5	223.1	25.	58.8
20.	298.0	9.	173.4	2.	1.0	292.4	20.	63.7
15.	346.7	8.	186.6	1.	.5	464.2	15.	70.6
10.	429.2	7.	202.8	.9	.45	497.9	10.	81.6
9.	453.7	6.	223.4	.8	.4	538.6	5.	104.5
8.	482.7	5.	250.3	.7	.35	588.8	4.	113.1
7.	517.9	4.	287.8	.6	.3	652.5	3.	125.4
6.	561.6	3.	344.5	.5	.25	736.8	2.	144.9
5.	618.2	2.	443.8	.4	.2	855.0	1.	185.6
4.	695.2	1.	684.5	.3	.15	1035.7	.75	205.7
3.	808.9	.9	731.1	.2	.1	1357.2	.50	237.7
2.	1001.3	.8	786.9	.15	.075	1644.1	.25	304.5
1.	1442.1	.7	855.4	.1	.05	2154.4	.15	365.5
.9	1524.3	.6	941.9	.09	.045	2311.2	.05	541.0
.8	1621.8	.5	1055.6	.08	.04	2500.0	.025	693.0
.7	1739.9	.4	1213.6	.07	.035	2732.8	.005	1231.3
.6	1886.9	.3	1452.6	.06	.03	3028.5		
.5	2077.0	.2	1871.6	.05	.025	3240.0		
.4	2335.8	.15	2240.3	.04	.02	3968.5		
.3	2717.7	.10	2886.4	.03	.015	4807.5		
.2	3364.1	.05	4451.4	.02	.01	6299.6		
.15	3914.1			.01	.005	10000.0		
.1	4845.2							
.05	6978.3							

only for the near-surface case of a surface blast. In stiff soil, ground motions from a surface blast will attenuate with depth.

Figures 14 and 15 give ground acceleration contours for a 15T TNT equivalent surface explosion at J5. The ground acceleration contours for a 50T TNT equivalent surface explosion at the proposed LARC are shown in Figs. 16 and 17.

Ground velocity contours for a 15T TNT equivalent surface explosion at J5 are shown in

Fig. 18. Figure 19 displays the ground velocity contours for a 50T TNT equivalent surface explosion at the proposed LARC.

Contours of ground displacement for a 15T TNT equivalent surface explosion at J5 are shown in Fig. 20. Displacement contours for a 50T TNT equivalent surface explosion at the proposed LARC are shown in Fig. 21.

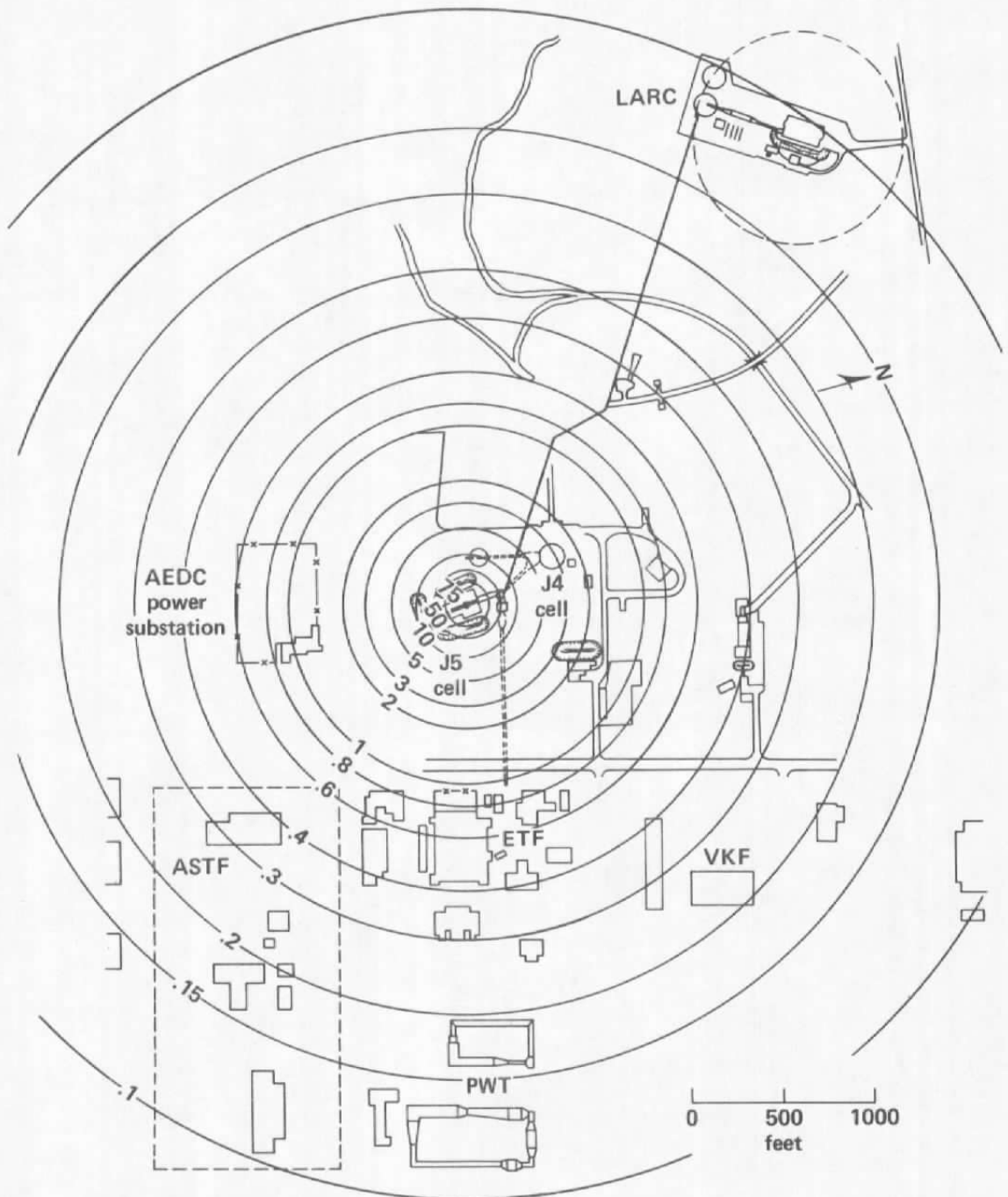


Figure 14. Near-source peak vertical acceleration contours (in g) for a 15T TNT equivalent surface explosion at J5.

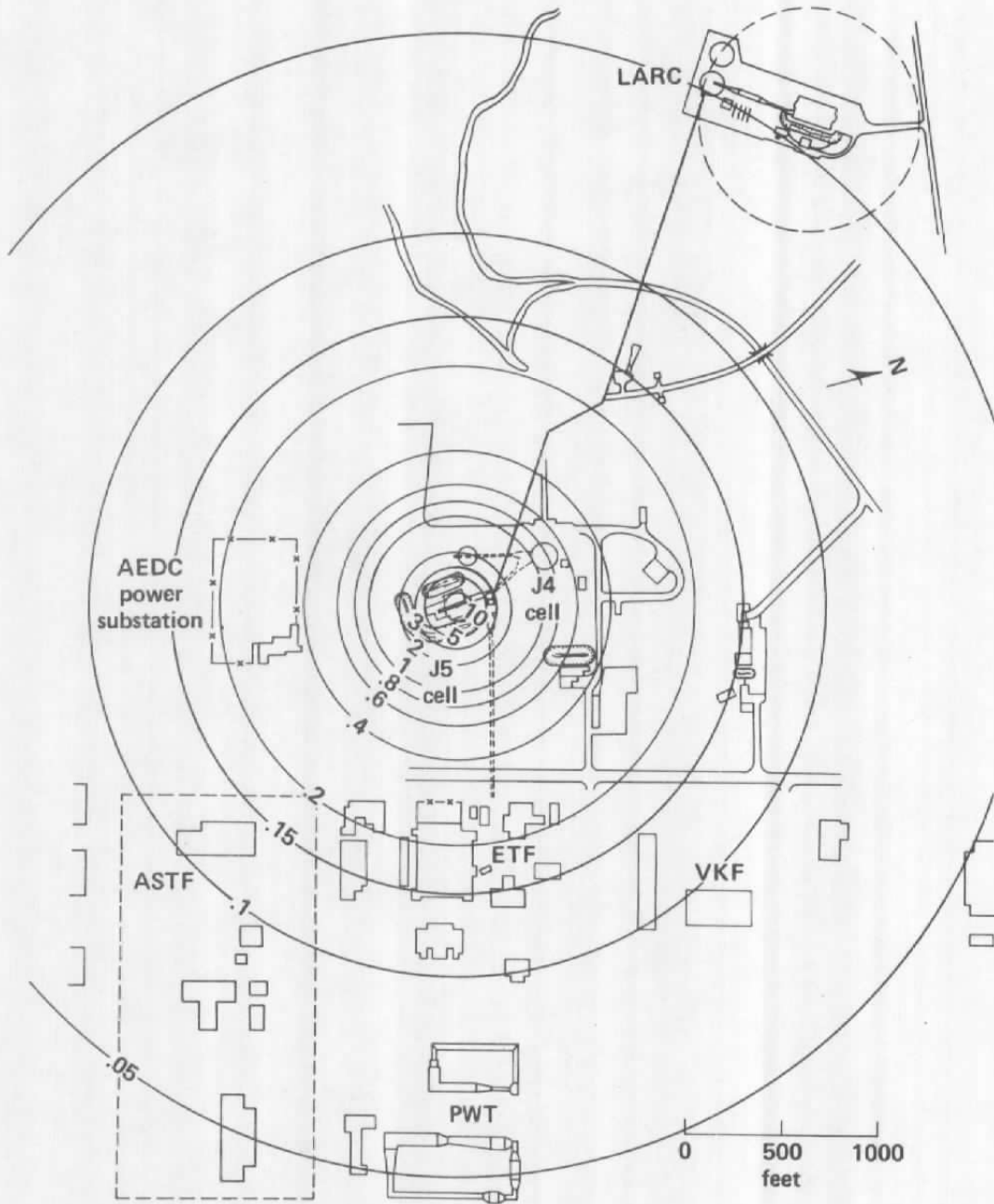


Figure 15. Near-source peak horizontal acceleration contours (in g) for a 15T TNT equivalent surface explosion at J5.

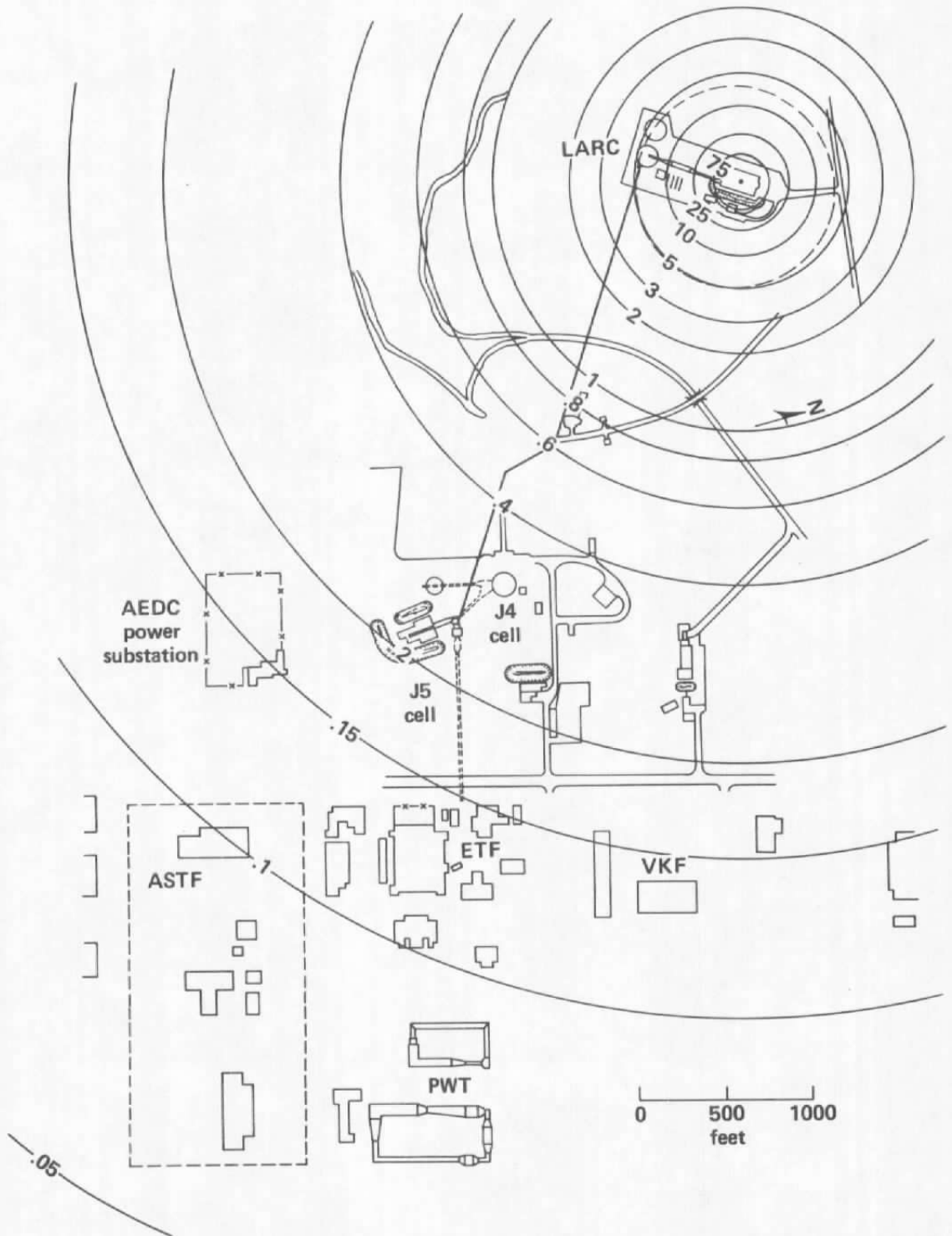


Figure 16. Near-source peak vertical acceleration contours (in g) for a 50T TNT equivalent surface explosion at the proposed LARC.

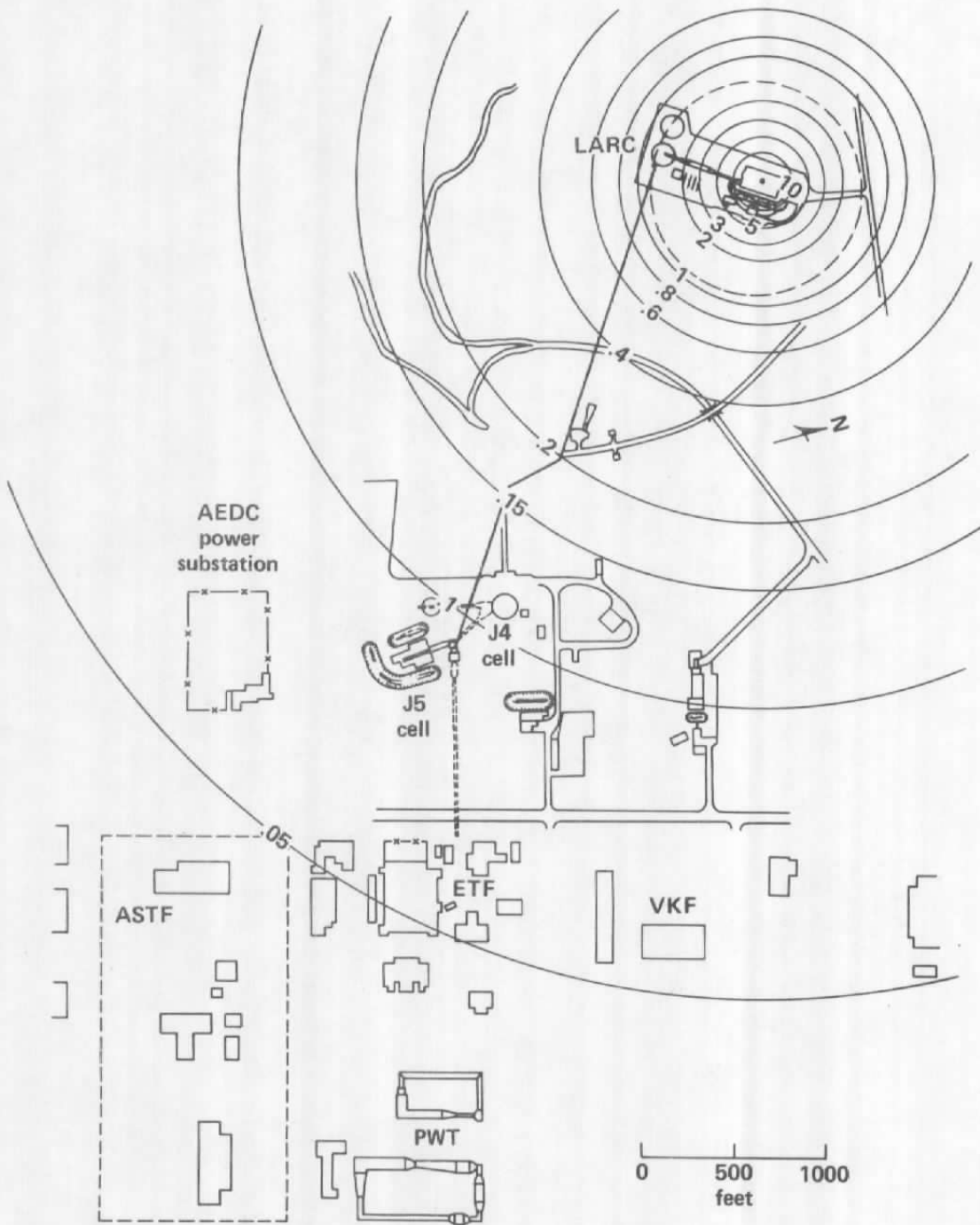


Figure 17. Near-source peak horizontal acceleration contours (in g) for a 50T TNT equivalent surface explosion at the proposed LARC.

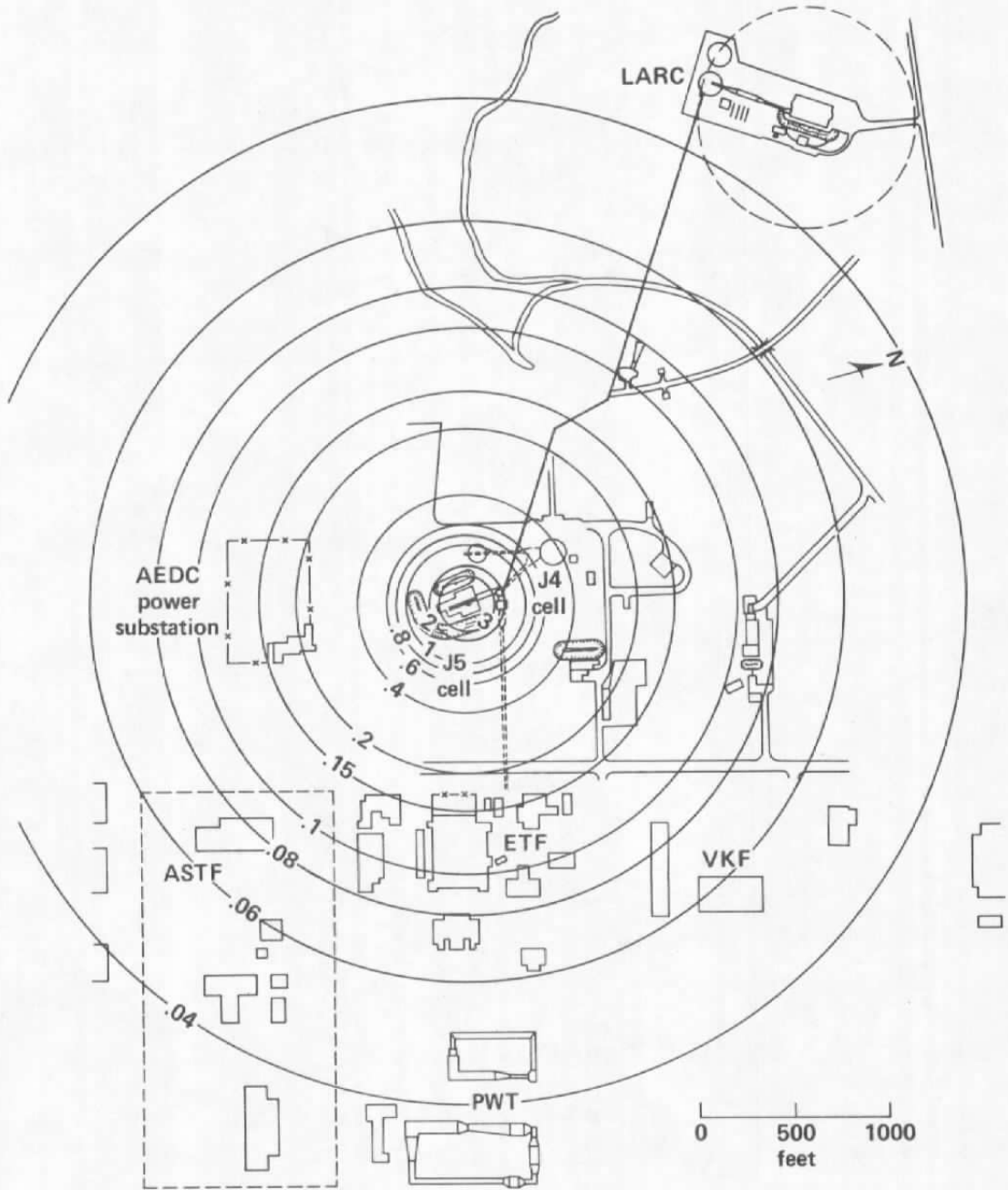


Figure 18. Near-source peak vertical velocity (horizontal velocity, $v_h = 0.5 v_v$) contours (in fps) for a 15T TNT equivalent surface explosion at J5.

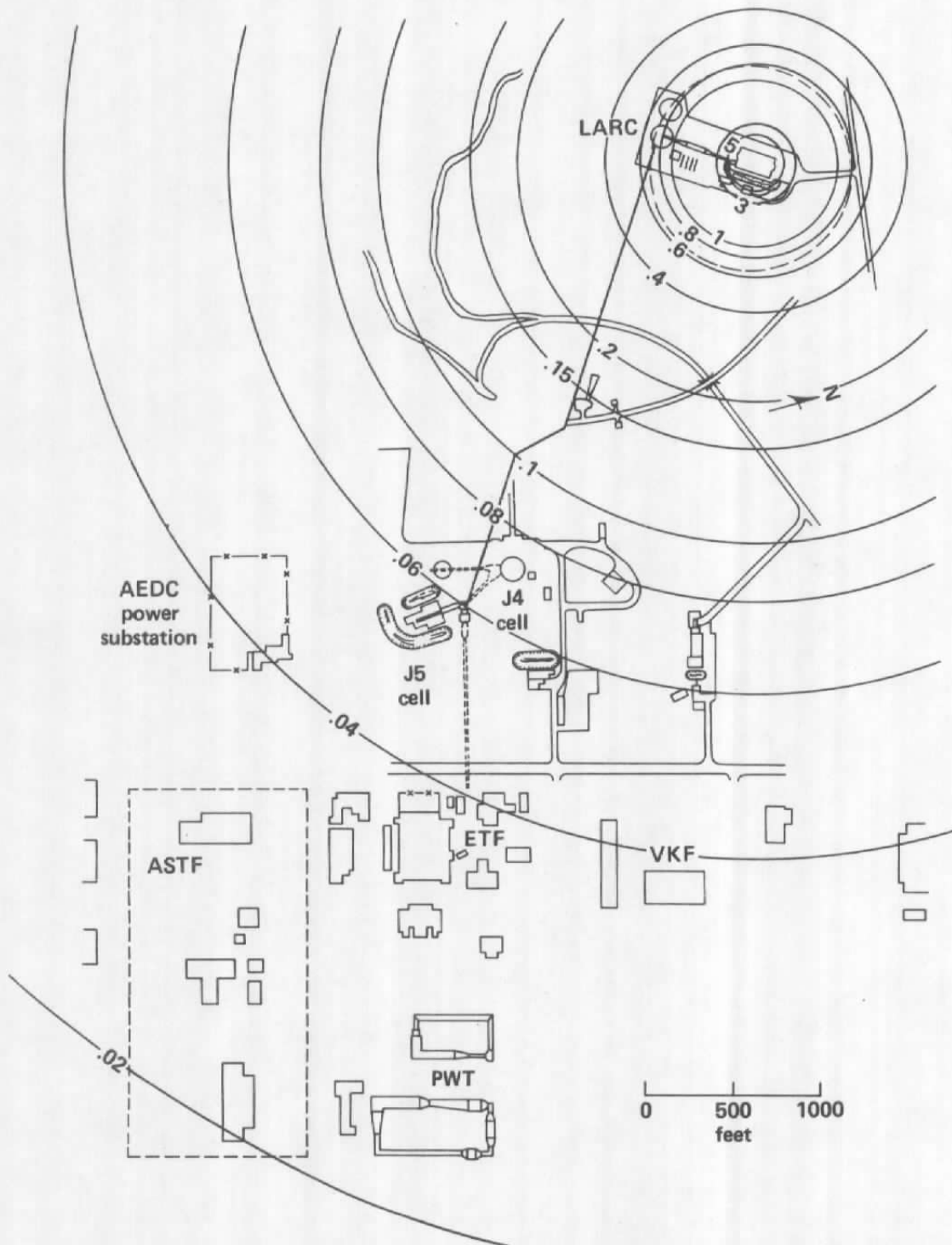


Figure 19. Near-source peak vertical velocity (horizontal velocity, $v_h = 0.5 v_v$) contours in fps for a 50T TNT equivalent surface explosion at the proposed LARC.

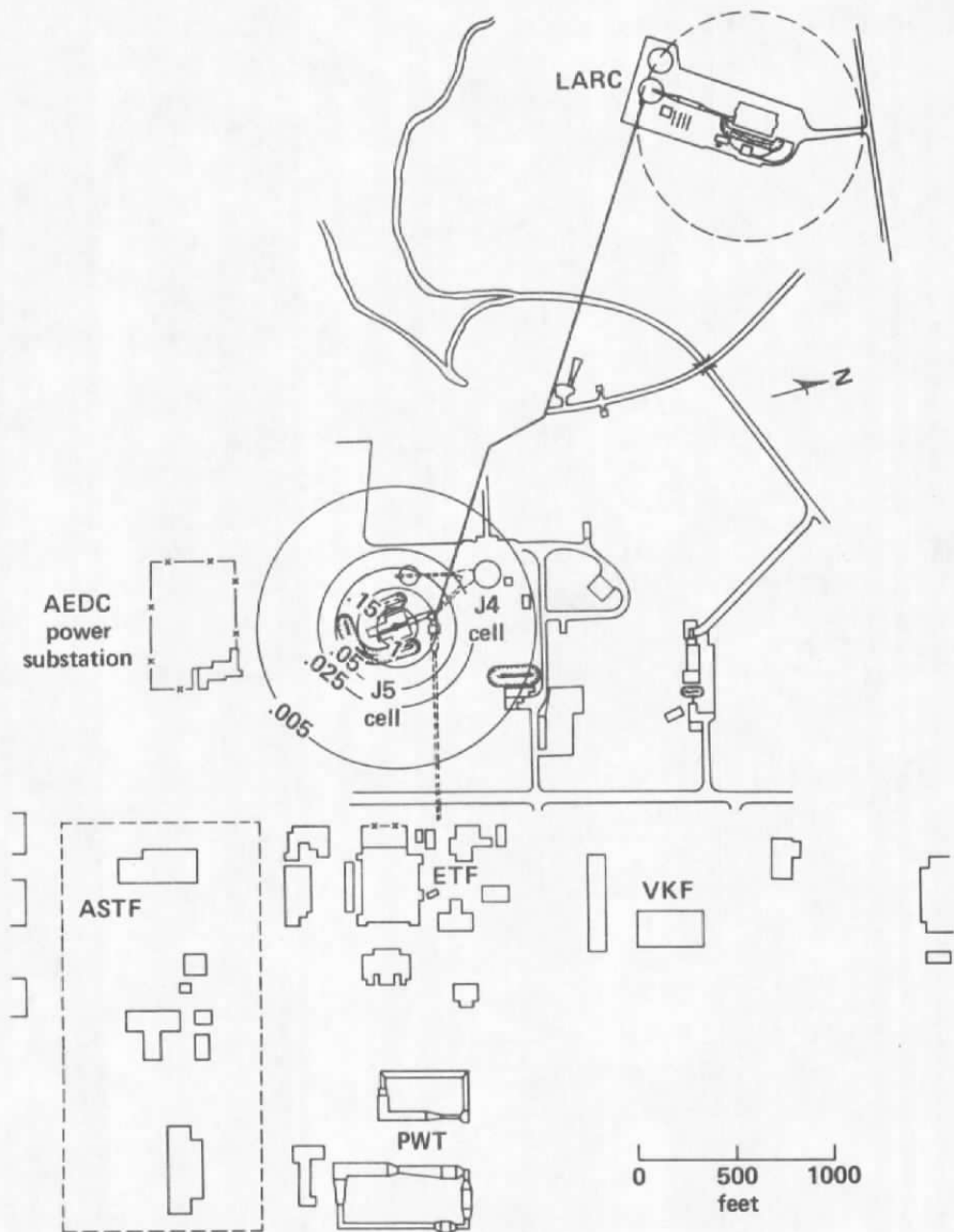


Figure 20. Near-source peak vertical or horizontal displacement contours (in in.) for a 15T TNT equivalent surface explosion at J5.

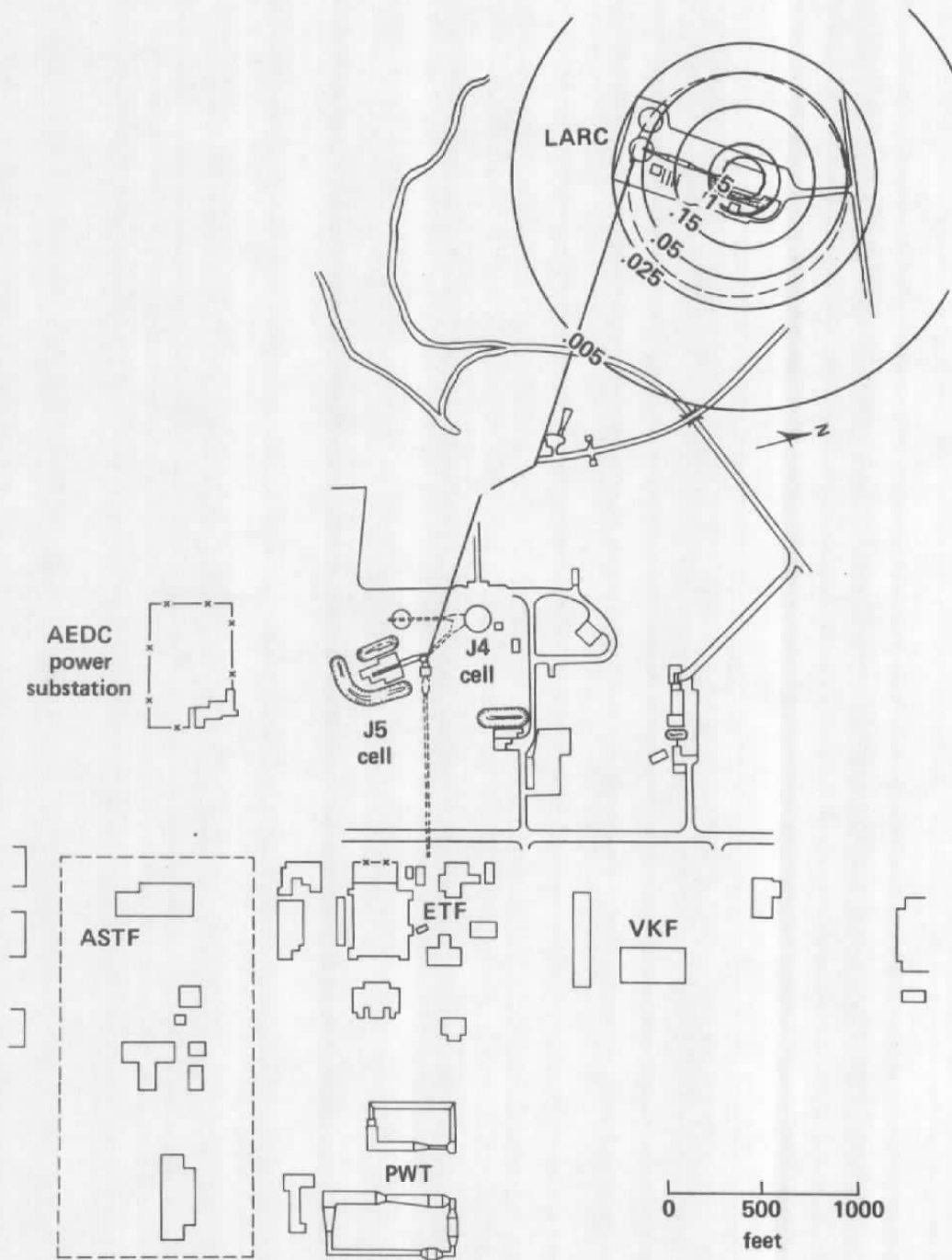


Figure 21. Near-source peak vertical or horizontal displacement contours (in in.) for a 50T TNT equivalent surface explosion at the proposed LARC.

Discussion of Damage Indicators

Maximum Acceleration as an Indicator of Damage

Some indication of average damage that may occur from ground shock can be gleaned from earthquake damage studies. Figure 22 gives average damage versus earthquake intensity for ten construction types. Intensity levels for an acceleration can be generated using Fig. 23.⁹

For the AEDC complex, these figures can be used to estimate average damage caused by ground acceleration. Ground acceleration can first be obtained from Figs. 14-17 at a specific location or structure. This maximum value can then be used to estimate earthquake intensity from Fig. 23. With the intensity value, Fig. 22 can be accessed to estimate average damage.

From examination of Figs. 14-17, it is seen that very high accelerations are predicted close-in. Because of the nature of the explosion that may occur at J5 or the proposed LARC, it is felt that the accelerations bias ground motion concerns. Earthquake studies of damage have generally found that long duration with low g can be more damaging than short duration of high g. These studies have also found that long-period ground motion can selectively damage taller or multistory buildings while leaving smaller buildings undamaged. The high accelerations may occur but are of short duration. The majority of the motion will be long period, low frequency. Figure 24 shows typical near-surface acceleration ground motions. Typical near-surface velocity ground motions are shown in Fig. 25. Table 5 lists the peak acceleration or velocity ground motions with range and the approximate duration of the ground motions for the DISTANT PLAIN events referenced. Since duration is relatively short, velocity is a better indicator of damage.

Maximum Velocity as an Indicator of Damage

Studies of blast damage have resulted in the establishment of threshold values of velocity for damage to ordinary dwellings. Duvall and Fogelson¹⁰ found that no damage occurred for $v \leq 2.0$ ips ($v \leq .167$ fps) and that major damage occurred for $v > 5.4$ ips ($v > .450$ fps). They recommend that only two zones be established, a safe zone and a damage zone, where 2 ips (.167 fps) separate the zones. Edwards and Northwood¹¹ report that no damage occurs for $v < 4.3$ ips ($v < .358$ fps) and that major damage occurs for $v \geq 9.0$ ips ($v \geq .750$ fps). The Duvall and Fogelson criteria are based on a data "pool" so that their values encompass a wide variety of structure types on different foundation materials. The Edwards and Northwood criteria are based only on six structures, half situated on wet, silty, clay soil, the others on well-consolidated glacial till. The structures were either frame or brick, all with stone masonry basements. The values they came up with are often used as guidelines for damage, but a review of their data indicates poor correlation and large standard deviation.

Empirical correlations developed by Trifunac and Brady¹² can be used to relate peak velocity to Modified Mercalli Intensity (MMI). Their 50 percent confidence level correlations of peak horizontal velocity at a stiff soil site to MMI are given in Table 6. These intensity values can be used in conjunction with Fig. 22 for an estimate of average damage per construction type. It can be seen that the empirical velocity-intensity correlation for earthquake damage compares well with the Duvall and Fogelson criterion for blast damage given above.

Recommendations

It is recommended that $v = 2$ ips ($v = .167$ fps) be used as a lower bound for an indication of structural blast damage. This correlates to a ground acceleration of 0.15 to 0.25 g.

Further discussion on use of these ground shock estimates has been included in the design criteria document prepared for use at the AEDC site.¹³

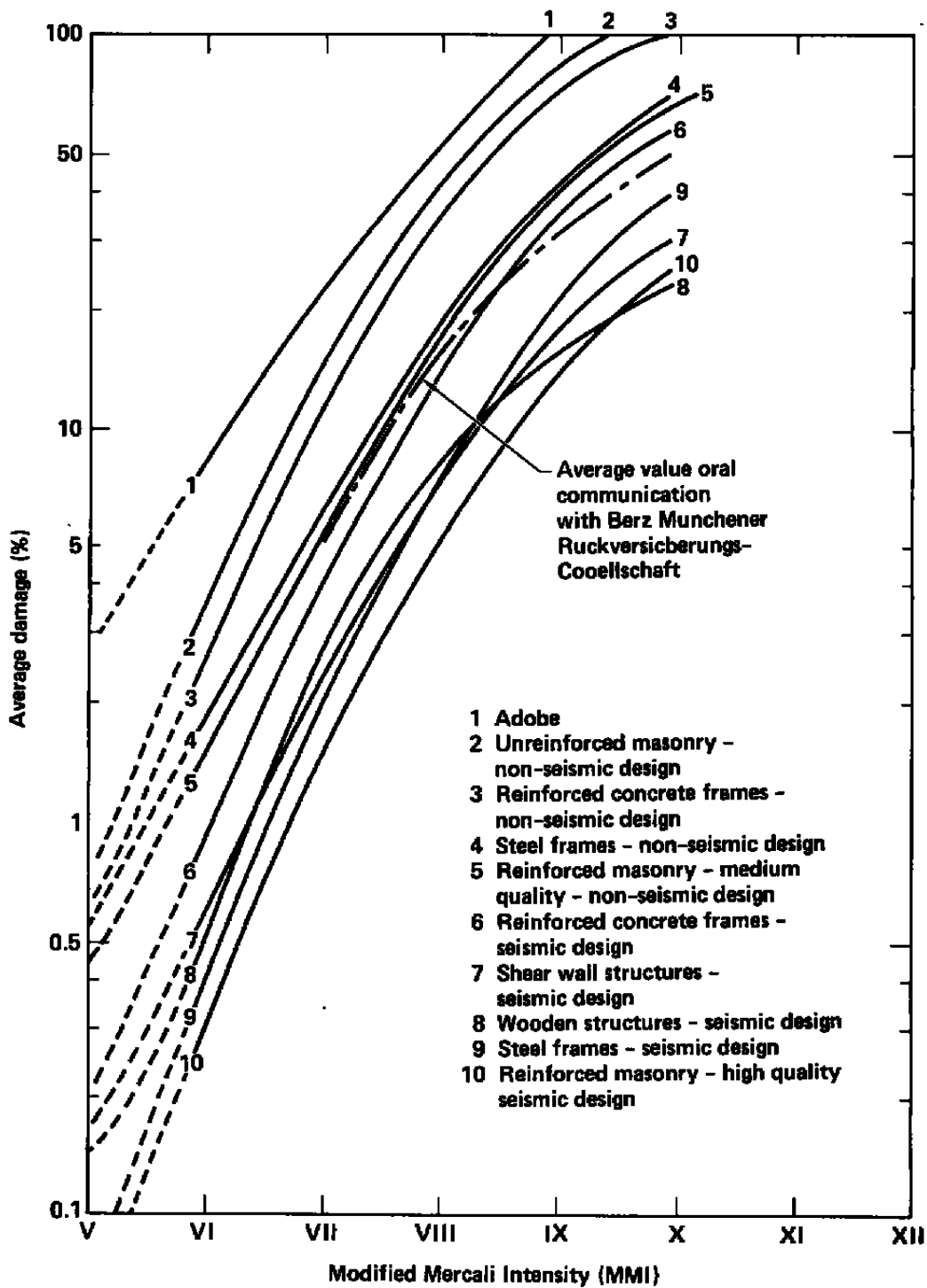


Figure 22. Average damage versus intensity (MMI) for ten construction types.⁹

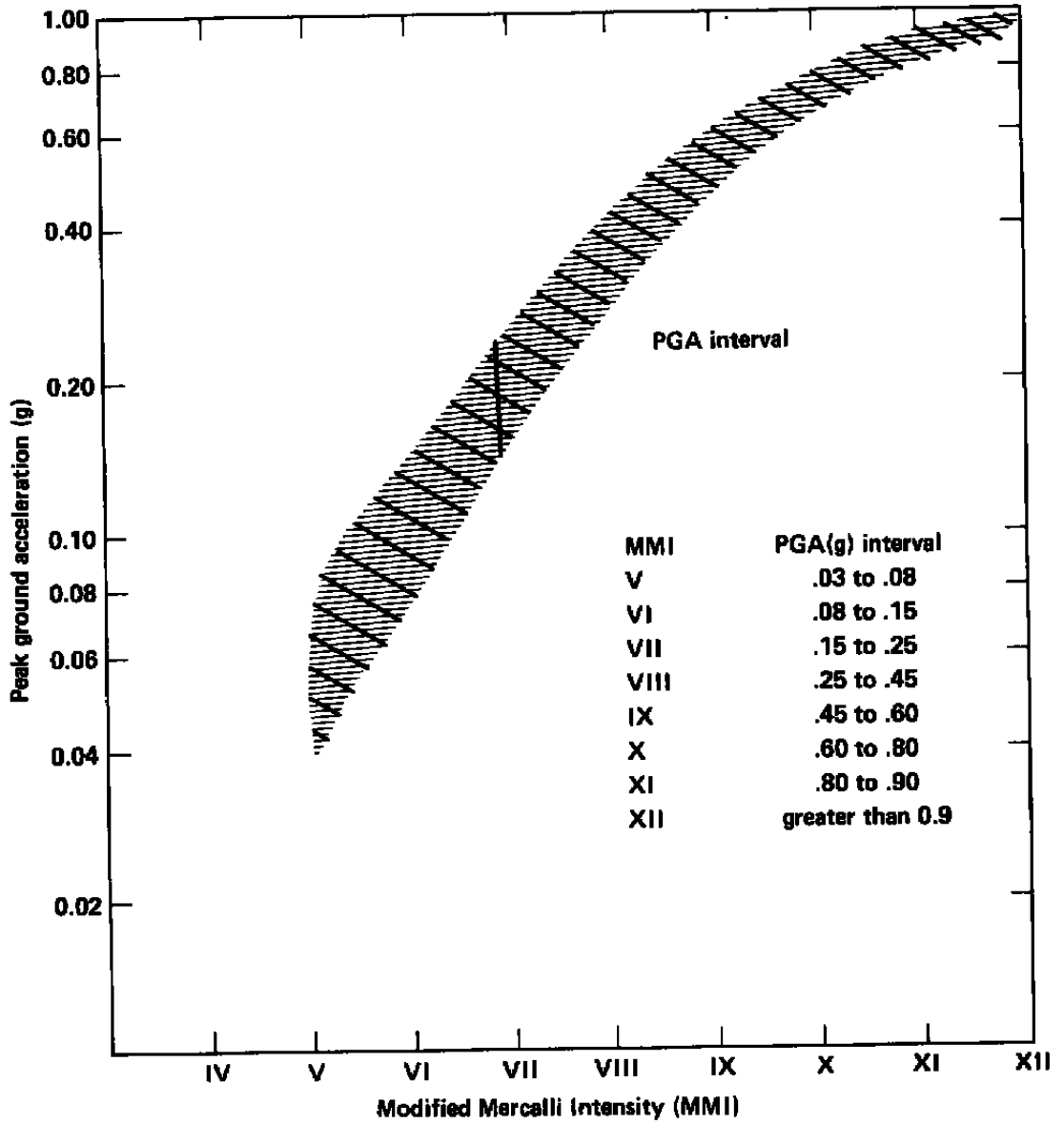


Figure 23. Modified Mercalli Intensity (MMI) relationship to peak ground acceleration.⁹

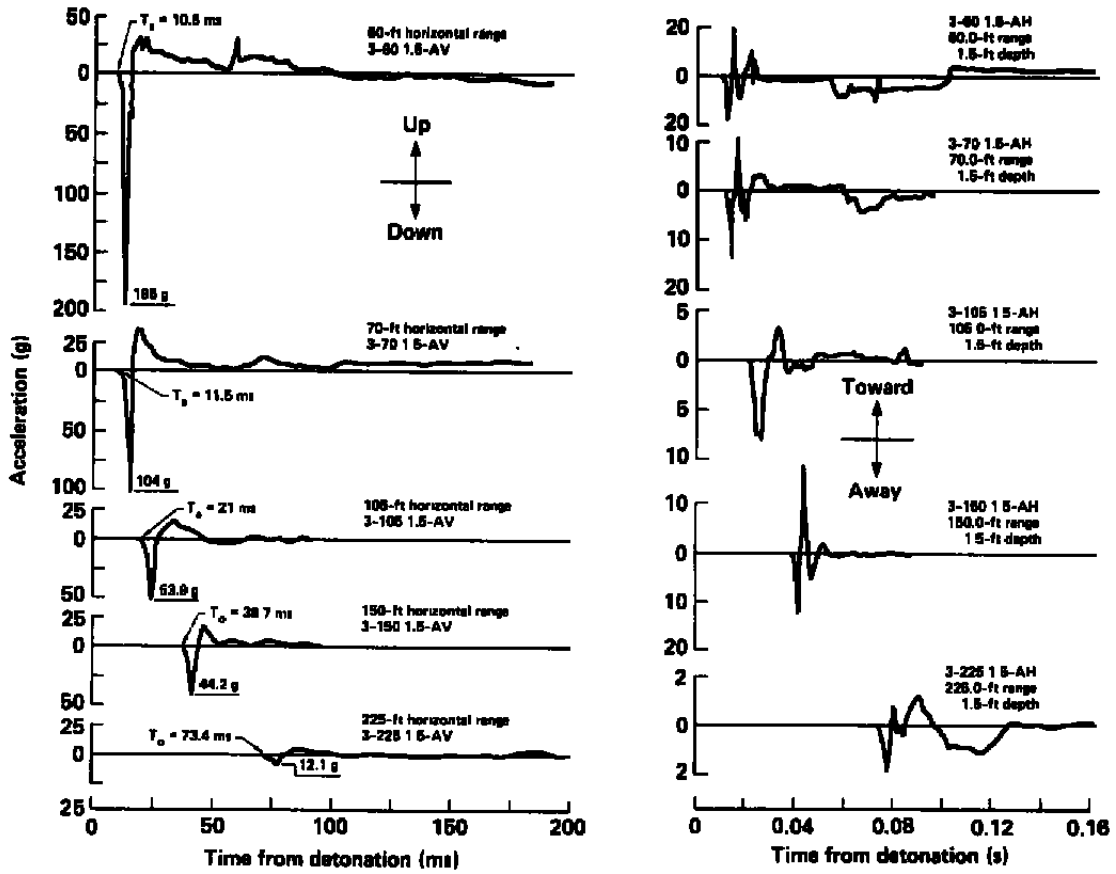


Figure 24. Accelerations, DISTANT PLAIN 3 (20T TNT equivalent surface blast).

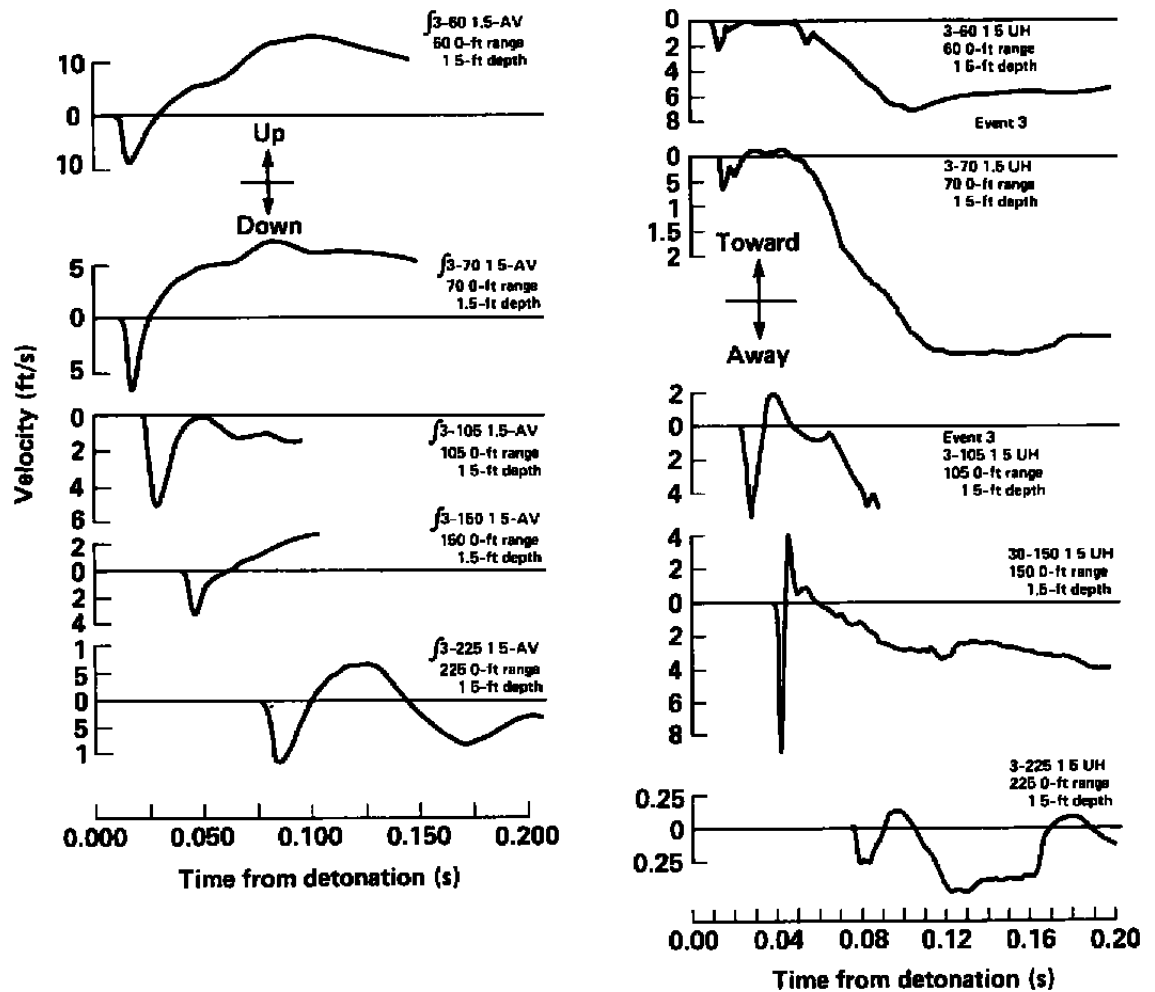


Figure 25. Velocities, DISTANT PLAIN 3 (20T TNT equivalent surface blast).

Table 5. Near-surface peak acceleration or velocity magnitudes and duration of the ground motions for DISTANT PLAIN Events referenced.

Event	Range (ft)	Ground motion parameter with associated duration			
		a_v (g)	t_d (ms)	a_h (g)	t_d (ms)
2A*	50	702.0	15.6	58.3	100.0
	80	191.0	27.5	10.6	75.0
	95	124.0	82.5	11.7	112.5
	125	95.9	47.5	22.6	100.0
	210	38.7	99.2	5.5	102.5
	390	7.0	87.5	4.2	102.5
3*	60	195.0	83.1	18.7	92.0
	70	104.0	90.3	14.0	84.0
	105	53.9	73.6	8.0	68.0
	150	44.2	68.9	12.3	44.0
	225	12.1	123.5	1.9	62.0
4 + *	240	10.8	175.0	4.9	200.0
	320	4.6	75.0	0.6	262.5
	450	6.1	325.0	1.2	325.0
	700	3.0	250.0	0.6	287.5
5*	60	165.0	66.3	34.4	80.0
	70	225.0	67.5	44.3	87.5
	105	58.3	52.5	10.0	20.0
	150	36.5	92.5	14.4	57.5
	225	20.4	115.0	3.4	57.5

Event	Range (ft)	Ground motion parameter with associated duration			
		v_v (fps)	t_d (s)	v_h (fps)	t_d (s)
6#	60	25.5	2.2	20.0	2.9
	80	29.0	1.4	7.9	2.2
	98	29.5	1.2	3.9	1.7
	140	22.0	0.8	2.1	1.1
	162	17.5	1.0	1.4	1.1

Notes: * DISTANT PLAIN 2A, 3, 4, and 5 measured acceleration; velocity arrived at from integrated acceleration.

+ DISTANT PLAIN 4 duration data are questionable.

DISTANT PLAIN 6 measured velocity; acceleration arrived at from differentiated velocity.

Table 6. Trifunac and Brady 50 percent confidence level correlation of peak horizontal velocity to Modified Mercalli Intensity (MMI) for a stiff soil site.

MMI	v_h	
	(ips)	(fps)
V	1.22	0.10
VI	2.37	0.20
VII	4.63	0.39
VIII	9.23	0.77
IX	18.00	1.50
X	35.09	2.92
XI	68.42	5.70
XII	133.40	11.12

References

1. C. Tirres and F. D. Cantrell, *A Proposed Large Solid Rocket Test Cell*, AIAA-84-0606, prepared for the AIAA 13th Aerodynamic Testing Conference, San Diego, CA (March 5-7, 1984).
2. R. E. Crawford, C. J. Higgins, and E. H. Baltmann, *The Air Force Manual for Design and Analysis of Hardened Structures*, Air Force Weapons Laboratory, Kirtland AFB, NM, AFWL-TR-74-102 (1974).
3. F. M. Sauer and J. E. Schoutens, "Volume IV, Part I—Empirical Analysis of Ground Motion from Above and Underground Explosions," *Nuclear Geoplosics Sourcebook*, DNA 6501H-4-1 (1979).
4. R. F. Flint and B. J. Skinner, *Physical Geology* (John Wiley & Sons, New York, 1977), 2nd ed., pp. 390-406.
5. SwRI, *A Manual for the Prediction of Blast and Fragment Loadings on Structures*, Southwest Research Institute, DOE/TIC-11268 (1980).
6. N. Lipner, D. C. Anderson, and P. K. Dai, *Ground Motion Environments for Generic Site Conditions*, TRW Systems Group, DNA 3872F (1975).
7. N. M. Newmark and J. D. Haliwanger, *Air Force Design Manual—Principles and Practice for Design of Hardened Structures*, Air Force Special Weapons Center, Kirtland AFB, NM, AFSWC-TDR-62-138 (1962).
8. F. M. Sauer, *Summary Report on DISTANT PLAIN Events 6 and 1a Ground Motion Experiments*, Stanford Research Institute, Menlo Park, CA, DASA-2587 (1970).
9. H. C. Shah, Purdue University, West Lafayette, IN, Class Notes for Earthquake Engineering and Seismic Hazard Analysis—CE 687 (Fall Semester 1981).
10. W. I. Duvall and D. E. Fogelson, *Review of Criteria for Estimating Damage to Residences from Blasting Vibrations*, U.S. Department of the Interior, Washington, DC, U.S. Bureau of Mines Report of Investigations 5968 (1962).
11. A. T. Edwards and T. D. Northwood, "Experimental Studies of the Effects of Blasting on Structures," *The Engineer*, v. 210 (September 30, 1960).
12. M. D. Trifunac and A. G. Brady, "On the correlation of seismic intensity scales with the peaks of recorded strong ground motion," *Bull. Seismol. Soc. Am.* 65 (1975).
13. SMA, *Design and Evaluation Criteria for Potential Motor Detonations at the Arnold Engineering Development Center (DRAFT)*, Structural Mechanics Associates, Newport Beach, CA, NTS/SMA 12211.03 (1984).

Bibliography

- Bollinger, G. A. (1980), *Blast Vibration Analysis*, Southern Illinois University Press, Carbondale and Edwardsville, IL.
- Ferritto, J. M., and J. B. Forrest (1975), *Ground Motions From Pacific Cratering Experiments 1000-Pound Explosive Shots*, TR-808, Civil Engineering Laboratory, Port Hueneme, CA.
- Hendron, A. J., Jr. (1975), "Engineering of Rock Blasting on Civil Projects," *Structural and Geotechnical Mechanics*, Prentice-Hall, pp. 242-277.
- Hendron, A. J., and C. H. Dowding (1974), "Ground and Structural Response Due to Blasting," *Advances in Rock Mechanics—Volume II, Part B*, Proceedings of the Third Congress of the International Society of Rock Mechanics, Denver, CO.
- Ingram, J. K. (1971), *Operation DISTANT PLAIN, Events 1, 2A, 3, 4, and 5; Project 3.02a, Earth Motion and Stress Measurements*, TR-N-71-3, U.S. Army Engineers Waterways Experiment Station, Vicksburg, MS.
- Jaramillo, E. E., and R. E. Pozega (1974), *MIDDLE GUST Free Field Data Analysis*, AFWL-TR-73-251, Air Force Weapons Laboratory, Kirtland AFB, NM.
- Langefors, U., and B. Kihlstron (1978), *The Modern Technique of Rock Blasting*, Third Edition, Halsted Press, John Wiley & Sons, New York, NY.
- Naar, J. (1964), "Part One—Theory of Directly-Induced Ground Motion," *Nuclear Geoplosics*, DASA-1285(1), Defense Atomic Support Agency, Washington, DC.

- Sandler, I. S., J. P. Wright, and M. L. Baron (1974), *Ground Motion Calculations for Events II and III of the MIDDLE GUST Series*, DNA 3290T, Weidlinger Associates, New York, NY.
- Trifunac, M. D. (1976), "A Note on the Range of Peak Amplitude of Recorded Accelerations, Velocities and Displacements with Respect to the Modified Mercalli Intensity Scale," *Earthquake Notes* 47(1).
- Wiegel, R. L. (Editor) (1970), *Earthquake Engineering*, Prentice-Hall, Inc., Englewood Cliffs, NJ.